Brus group experimental areas

1. Carbon Nanotube Excited States:
Two photon study of Excitons
Rayleigh Scattering for identification of single tubes
Short tubes in the interstellar medium?

2. Transition metal oxide nanocrystals and nanowires:
electric force microscopy
hydrothermal and organometallic synthesis
structural phase transitions

3. Local electromagnetic field enhancement around Ag Nanocrystals

Chemistry and Physics of Semiconductor Nanocrystals

Louis Brus
Chemistry Department
Columbia University

History
Synthesis and self-assembly into solids
Electronic Structure and Luminescence
Optical Spectra of Single Nanocrystals
Charge State of Single Nanocrystals.

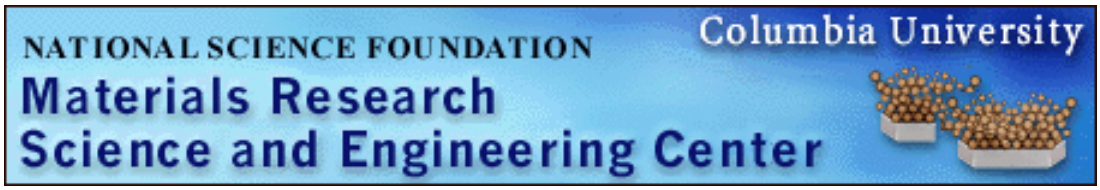

NSF Nanocenter on Electrical Conductivity of Single Molecules and Carbon Nanotubes

What is a CdSe nanocrystal?

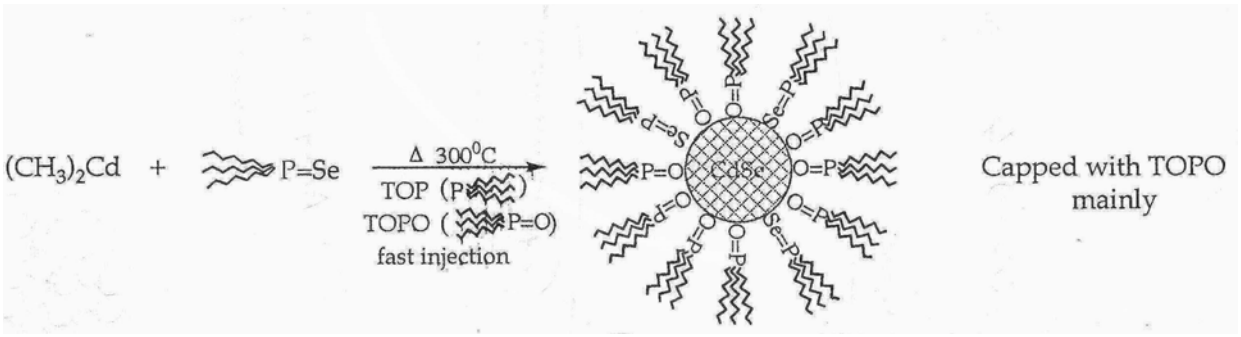

- Organic molecules ‘cap’ the outer surface of core semiconductor. They prevent aggregation, oxidation, and stabilize nanoparticles in the solution. Most important, they electronically isolate the particles and passivate the surface states.

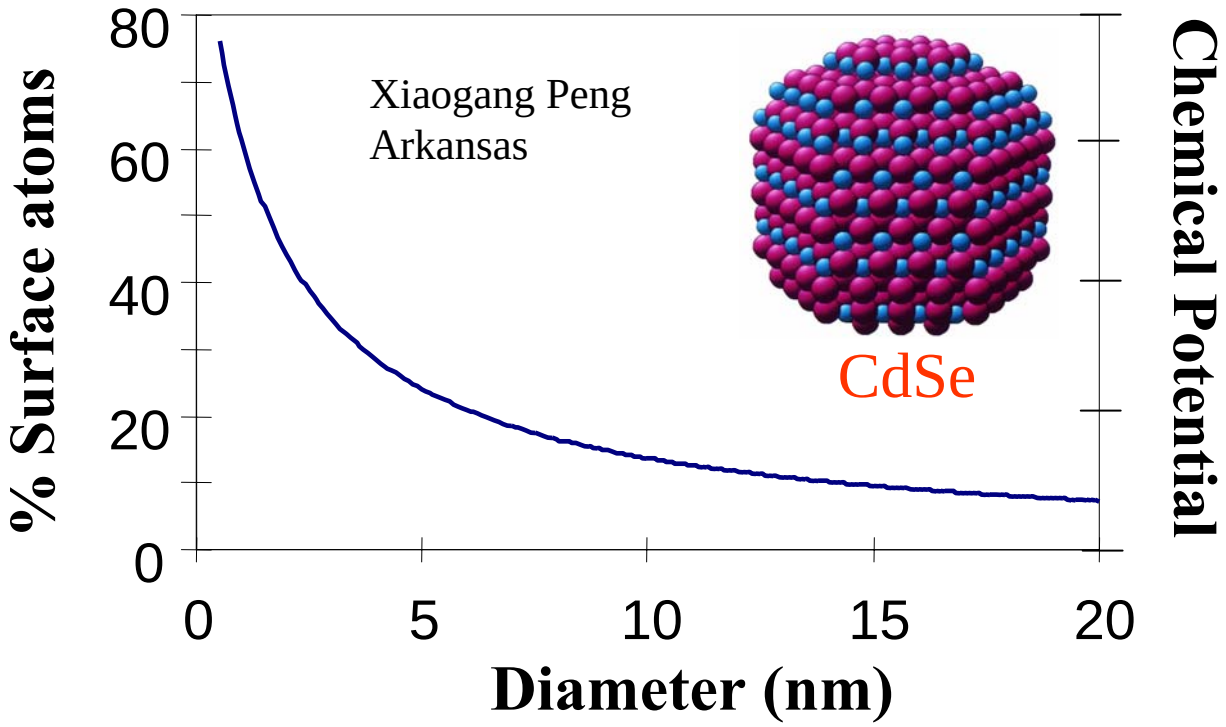

Journal of Chemical Physics 79, 1086 (1983)

1983

Quantum size effects in the redox potentials, resonance Raman spectra, and electronic spectra of CdS crystallites in aqueous solution

R. Rossetti, S. Nakahara, and L. E. Brus

Bell Laboratories, Murray Hill, New Jersey 07974
(Received 31 March 1983; accepted 5 May 1983)

We report observation of size effects in the excited electronic properties of small, crystalline CdS particles. We also theoretically model the leading small size correction terms applicable to the photochemical redox potentials and lowest exciton energy. Our experiment involves controlled formation of CdS crystallites in aqueous solution; the photophysics and surface redox chemistry of electrons e^- and holes h^+ in these colloidal crystallites has been of recent interest.[1-6]

Transmission electron microscope examination of particles from a freshly prepared colloid shows a narrow size distribution.[7] A typical particle diameter is $\simeq 35$ Å, which corresponds to about six unit cells. The mass weighted average diameter $\bar{d}$ is $\simeq 45$ Å. The particles are crystalline (cubic CdS), with moderate diffraction ring broadening due to small crystallite size. In colloidal solution, thermodynamics favors growth of larger crystallites at the expense of smaller ones. We observe that, if these colloids "age" for $\simeq 1$ day at pH 3, the size distribution becomes broader with $\bar{d} \simeq 125$ Å. On the average, 21 small crystallites dissolve and recrystallize onto one larger "seed" crystallite. The colloid remains transparent without CdS precipitation as it ages. The crystal structure is mixed cubic and hexagonal after aging; the hexagonal phase is thermodynamically more stable.

Resonance Raman (RR) spectroscopy[8] in principle allows an *in situ* vibrational characterization despite the low crystallite concentration $\simeq 2\times10^{-6}$ M in fresh colloids. The 416 nm RR spectrum in Fig. 1 shows the LO (longitudinal optical) phonon at 305 cm^{-1} and a weaker overtone near 605 cm^{-1}. These CdS peaks are superimposed on nearly continuous water Raman scattering. $e^- - h^+$ recombination luminescence has been largely quenched by addition of $\simeq 10^{-3}$ M benzoquinone.[3] At 395, 448, and 460 nm similar spectra are observed. To the red (480, 503, and 532 nm) and to the blue (355 and 266 nm), the CdS RR spectra are far weaker and not detected.

To our knowledge these are the smallest isolated crystallites that have been examined by Raman spectroscopy.[9,10] The LO peak occurs within a couple of cm^{-1} of the bulk CdS frequency. In Fig. 1 the low frequency wing, in the region of expected surface mode maxima,[11] is slightly stronger than the high frequency wing. In other fresh colloids, the LO peak is more symmetrical. Shifts and surface mode maxima have been reported for small crystalline grains in Si films.[12,13]

In aged colloids the CdS RR excitation spectrum changes markedly. RR scattering at 395, 416, and 448 nm is not detectable, with the cross section per unit mass decreasing by at least a factor of 10. Recall that there is no loss of CdS mass during aging; mass shifts from smaller to larger crystallites. CdS RR scattering is detected in the red shifted and narrower spectral range 463–480 nm. The spectra are similar to those in Fig. 1, with an LO peak decrease of $\simeq 3$ cm^{-1} and a slight narrowing.

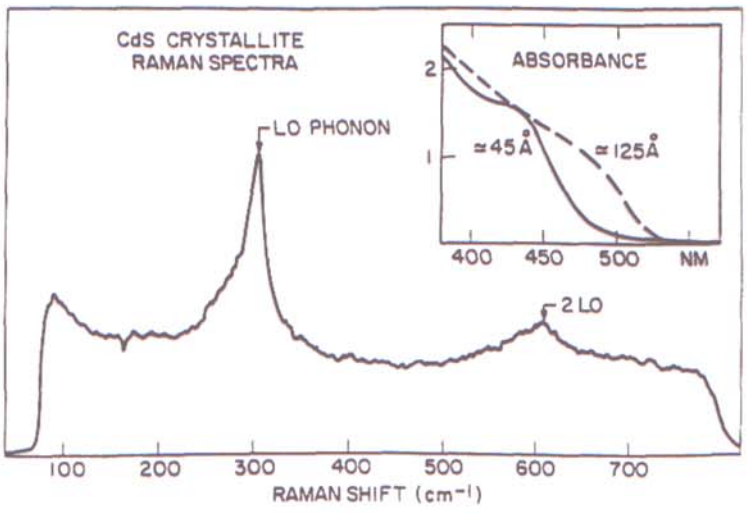

Synthesis 1986 Steigerwald etal, JACS 110, 3046 (1988)

Organometallic synthesis, controlled Growth, Surface "capping" and isolation of stabilized clusters

A] Take advantage of hydrocarbon phase – hydrophobic reagents

* Mike Steigerwald
Paul Alivisatos
Lou Brus

small 18 Å N≃70
large 50 Å N≃630
standard deviation 20%

dry → redisolve → heptane colloid

B] Controlled Growth

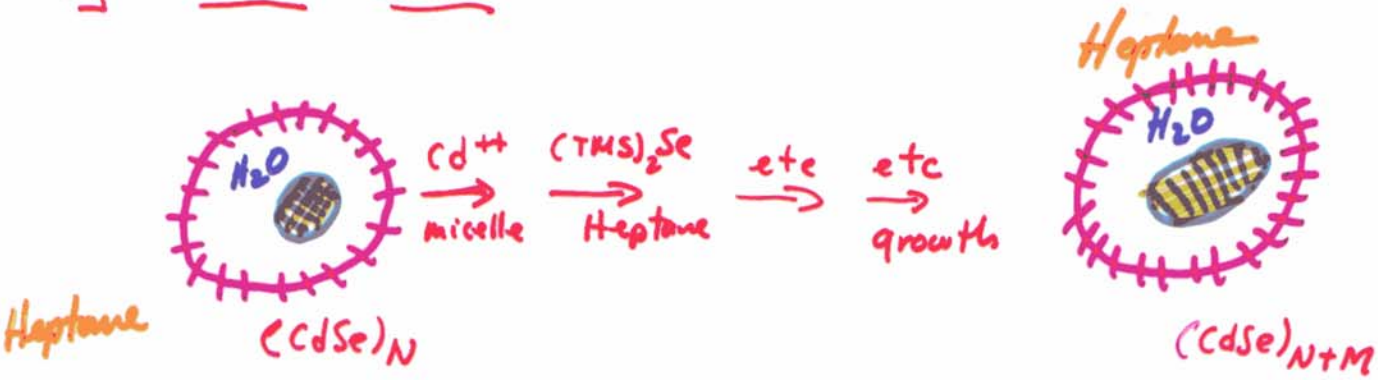

Crystallite in micelle, with water present, is stable yet can grow further

⟹ exotic chemistry on surface

⟹ concentric growth of one material on another

Synthesis 1988 Bawendi etal J. Chem. Phys. 91, 7282 (1989)

Two Step Organometallic Synthesis of CdSe Single Crystallites

(Mike Steigerwald)

(Moungi Bawendi)

1)

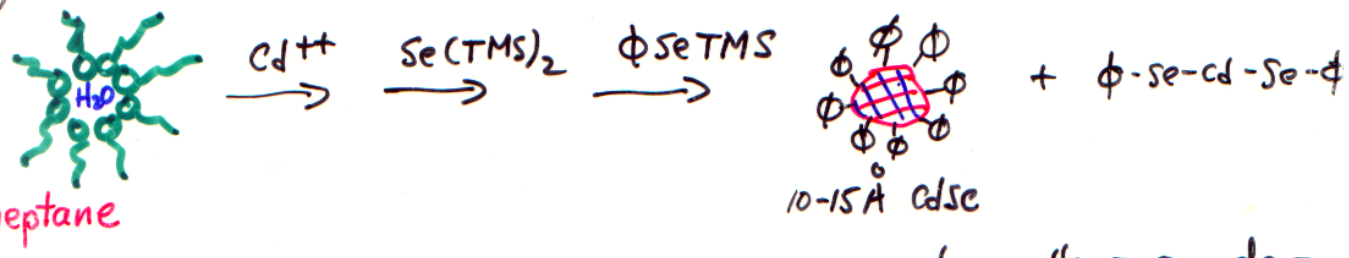

heptane

inverse micelle

pale yellow powder

2)

pale yellow powder

Reflux 230°C

3 hours

90% Bu_3P

10% Bu_3PO

Ar

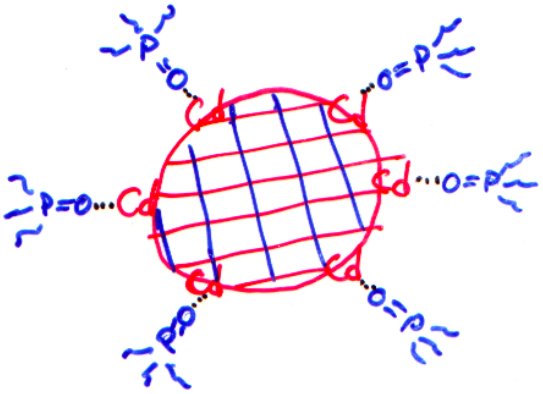

"capped 32 Å

clear red solution

fluorescence

Characterization

TEM	Pat Carroll
Powder x-ray	Refik Kortan
^{77}Se NMR	Peter Reynders
Se, Cd EXAFS	Matt Marcus

Chemical synthesis of CdSe nanocrystals

- Narrow size distribution (~5%) is obtained by the fast injection of the chemical reagents into the flask at high temperature (~ 350 ^{0}C).

- The precursors are prepared in the glove box to avoid oxygen and water.

Semiconductor: CdSe, CdTe, PbSe, etc.
Metal: PtFe

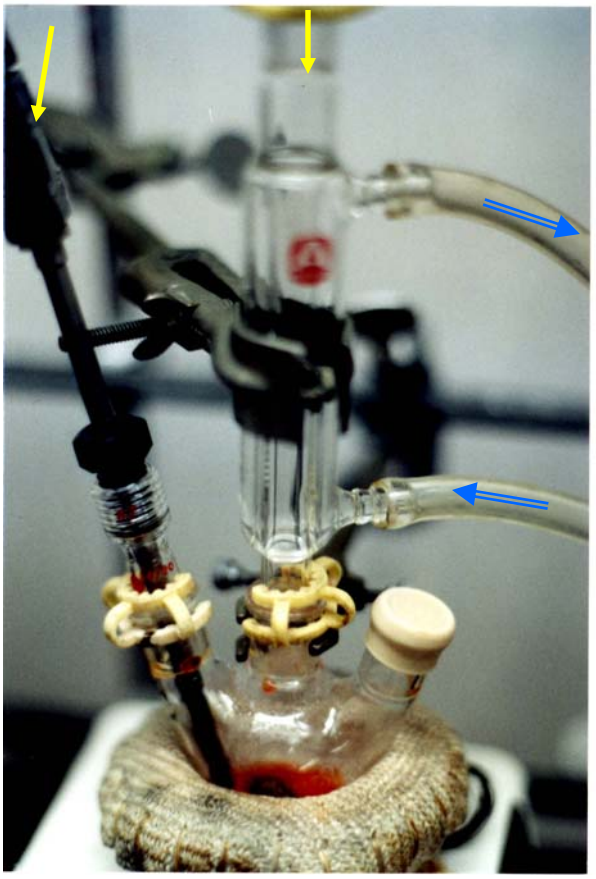

TEM of cubic PbSe nanocrystals

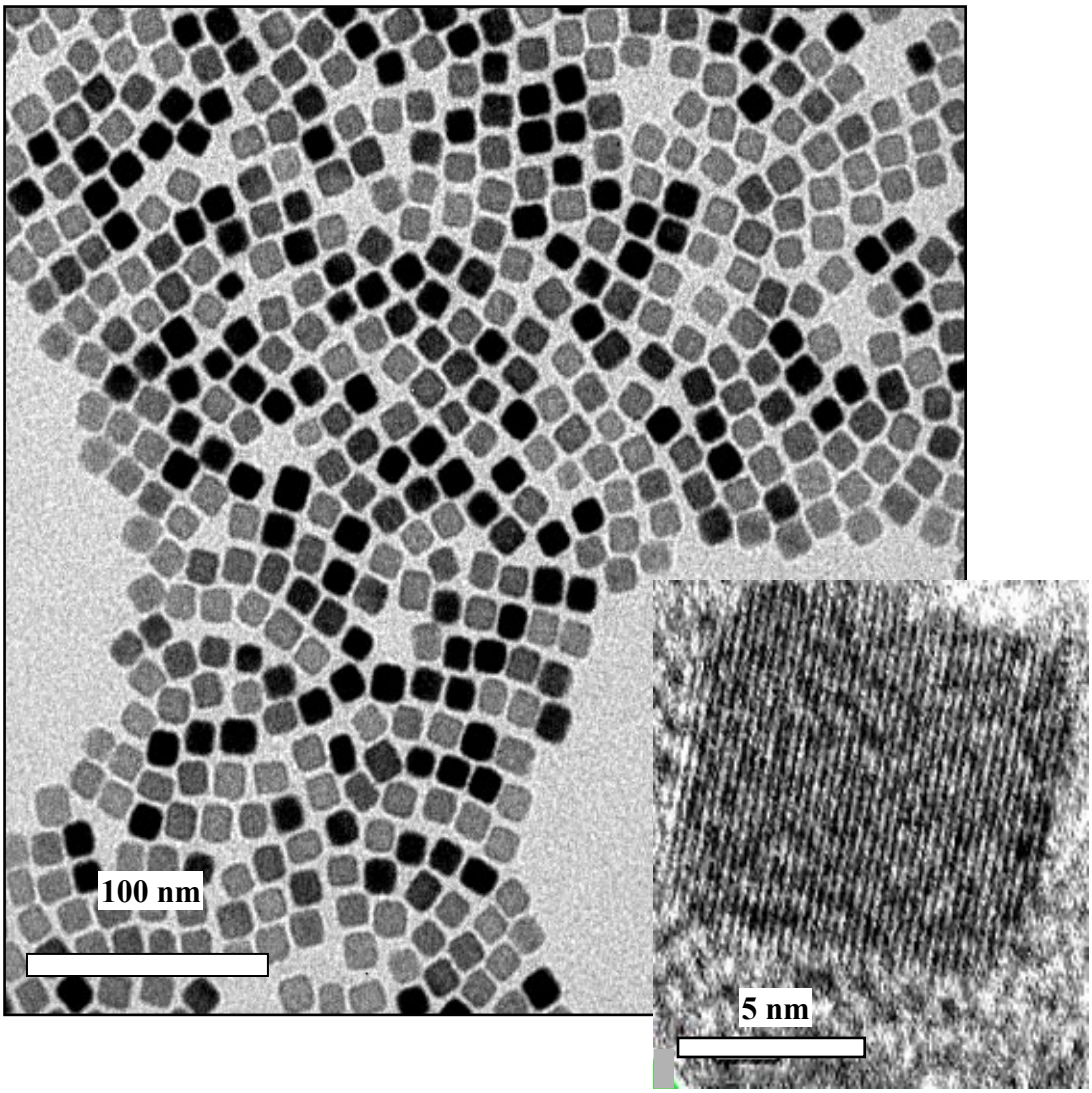

TEM images of PbSe quantum cubes after size selection (reaction temperature 215^{o}C), size ~12 nm

Change of shape from spheric to cubic in the size regime of 8 to 11 nm

Chris Murray, Wolfgang Gaschler, Franz Redl, IBM-Columbia

Low Temperature oganometallic Synthesis of TiO_2

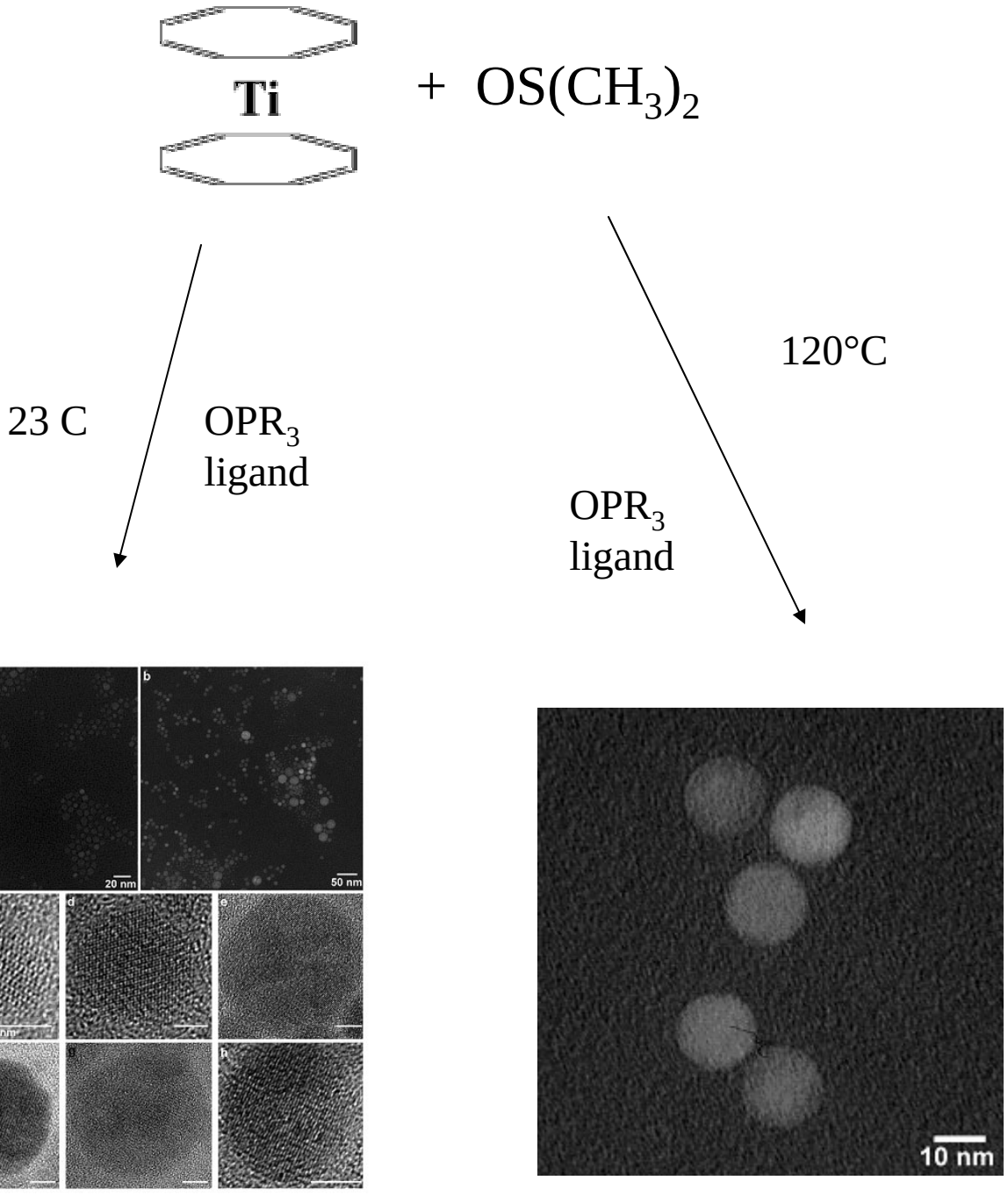

Jing Tang, Franz Redl, Yimei Zhu, Theo Siegrist, Louis E. Brus and Michael L. Steigerwald, "A Low-Temperature Synthesis of TiO2 Nanoparticles" , Nano Letters 5**,** 543-548 (2005).

Growth of wires and exotic shapes
With junctions between different materials

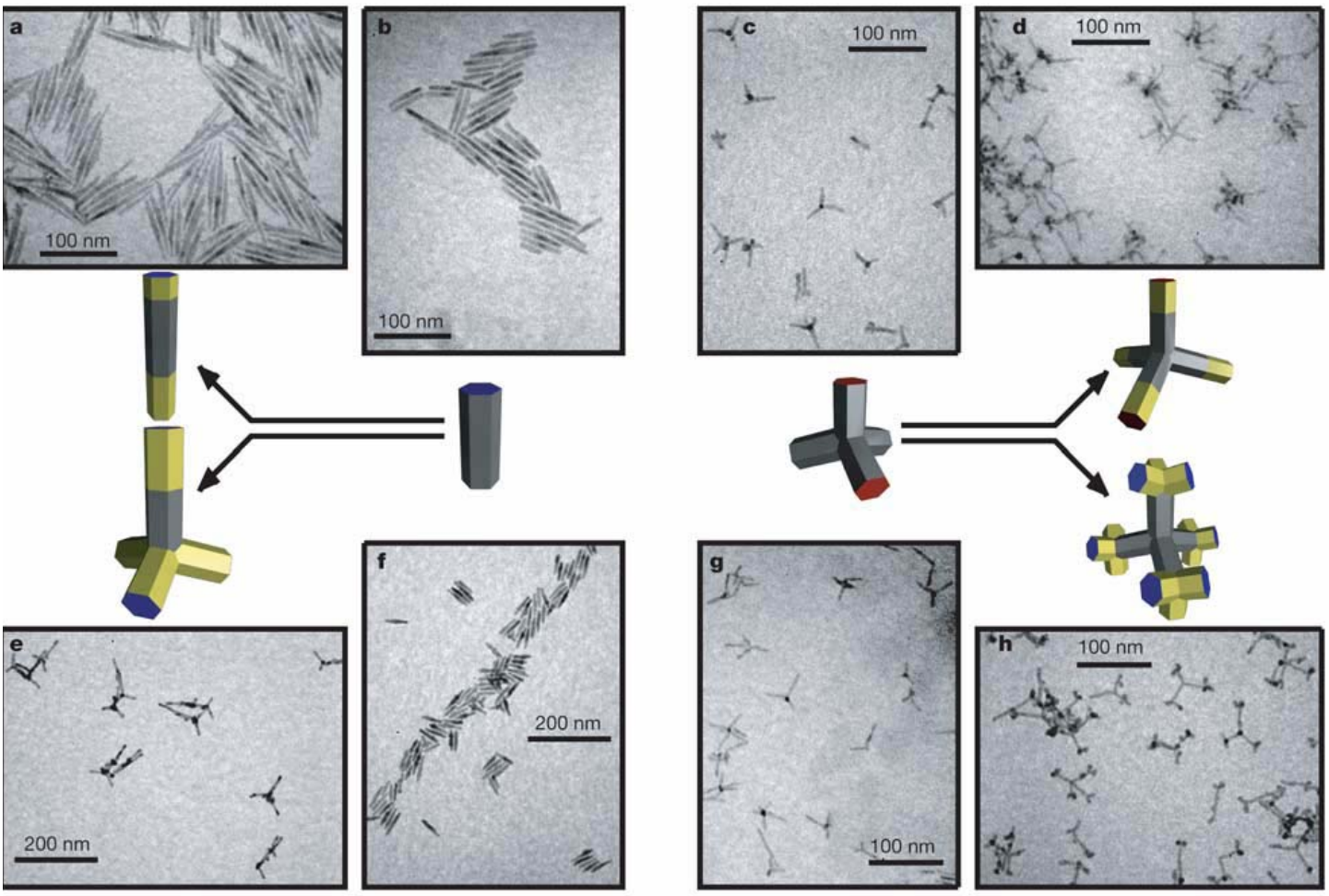

D. Milliron etal, Nature 430, 190 (2004) – Alivisatos Group

3D solid structures

Elena Shevchenko
O'Brien – Murray
Columbia-IBM

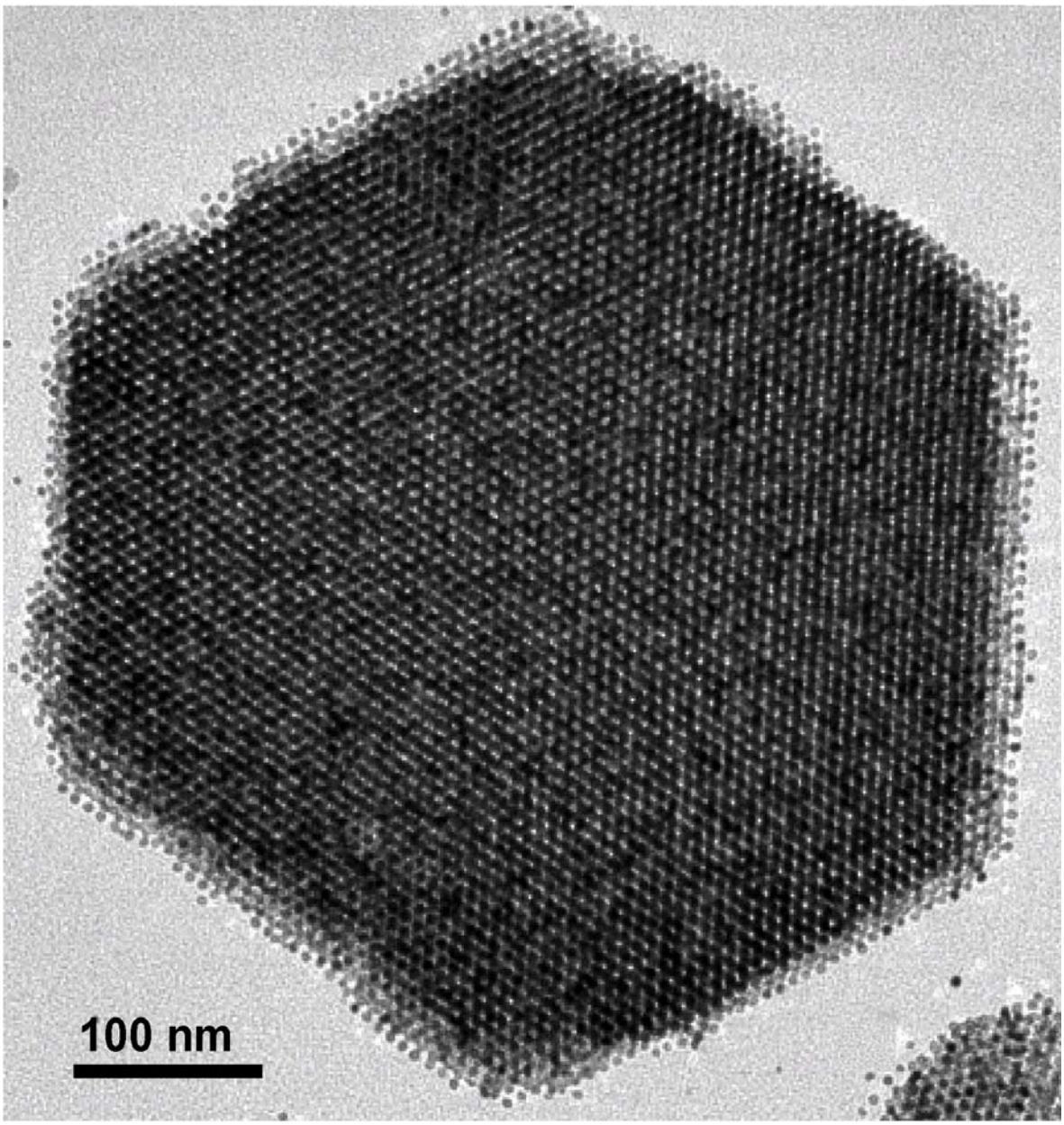

$CoPt_3$ nanoparticles

Bimodal superlattice of 11 nm magnetic Fe_2O_3 NCs and semiconducting 5 nm PbSe NCs

Redl, Cho, Murray, O'Brien Nature 423, 968 (2003)

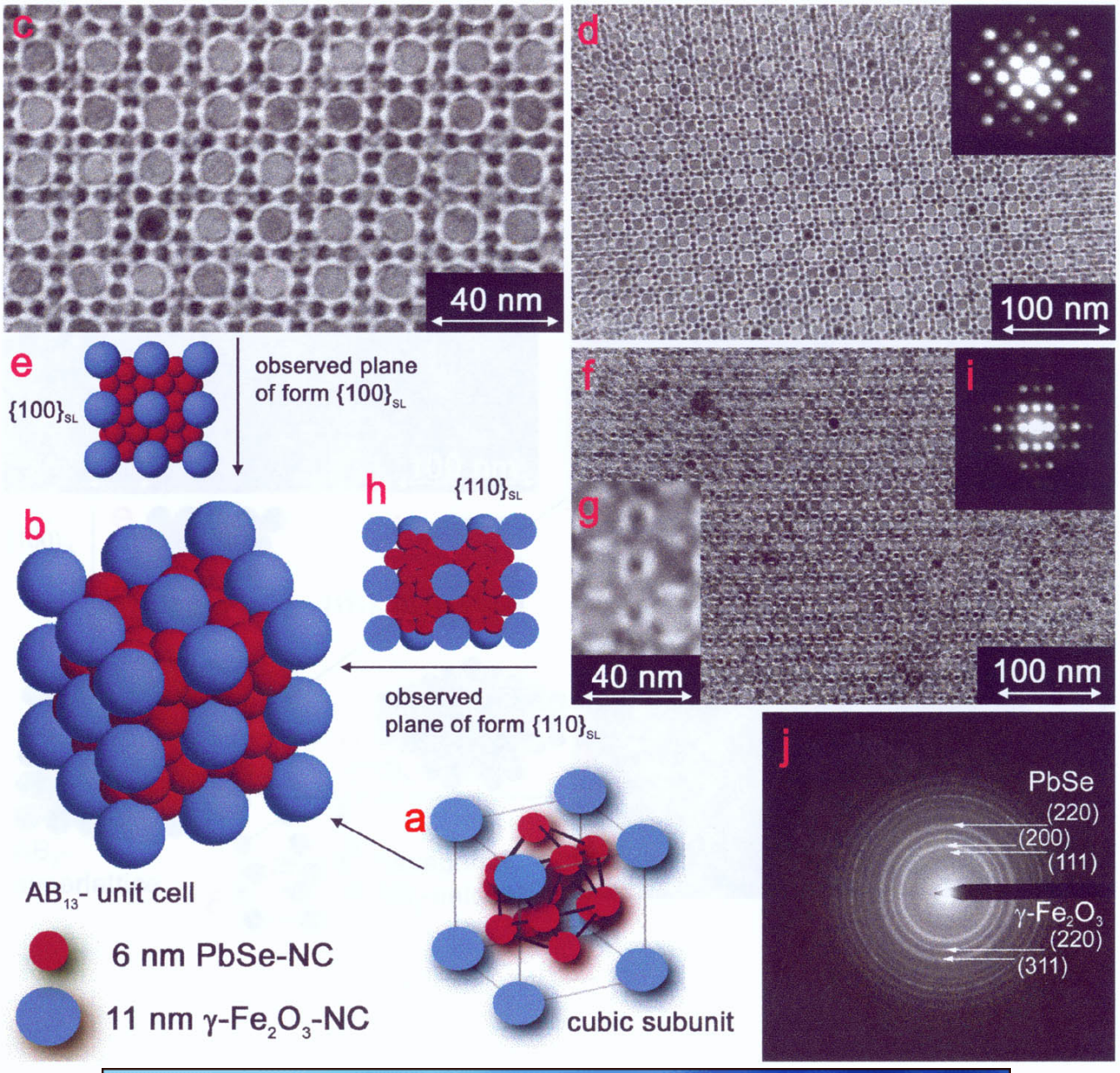

NATIONAL SCIENCE FOUNDATION
Materials Research Science and Engineering Center
Columbia University

CdSe Size Dependent Absorbance

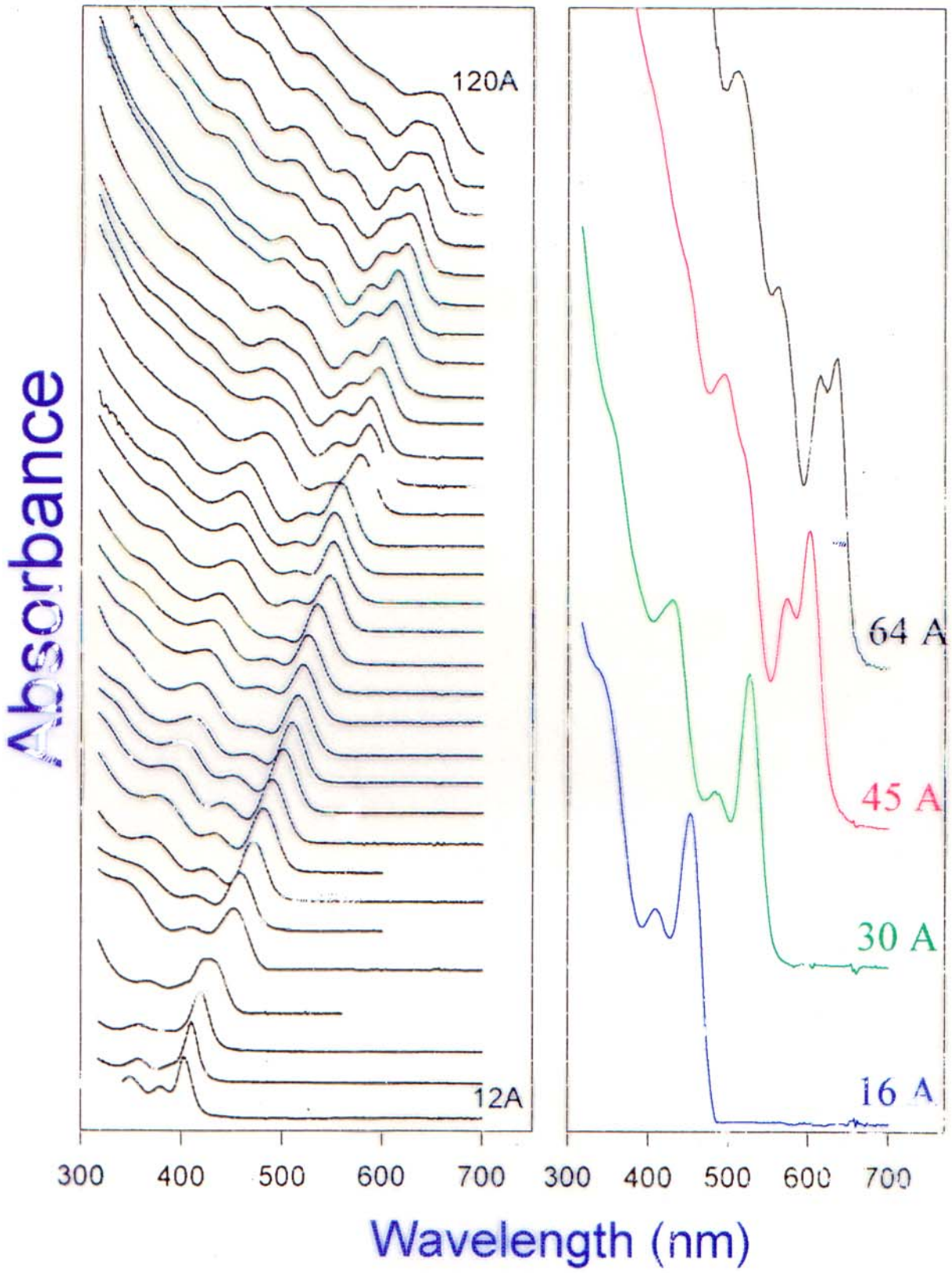

C. Murray and M. Bawendi

Chris Murray & Moungi Bawendi (MIT)

Size tunable luminescence
Narrow emission band

High Quantum Yield Luminescence
More stable than dye molecules
Possible use in biological imaging

ZnS surface shell layer “insulates” the luminescent CdSe core

high quantum yield and photostability

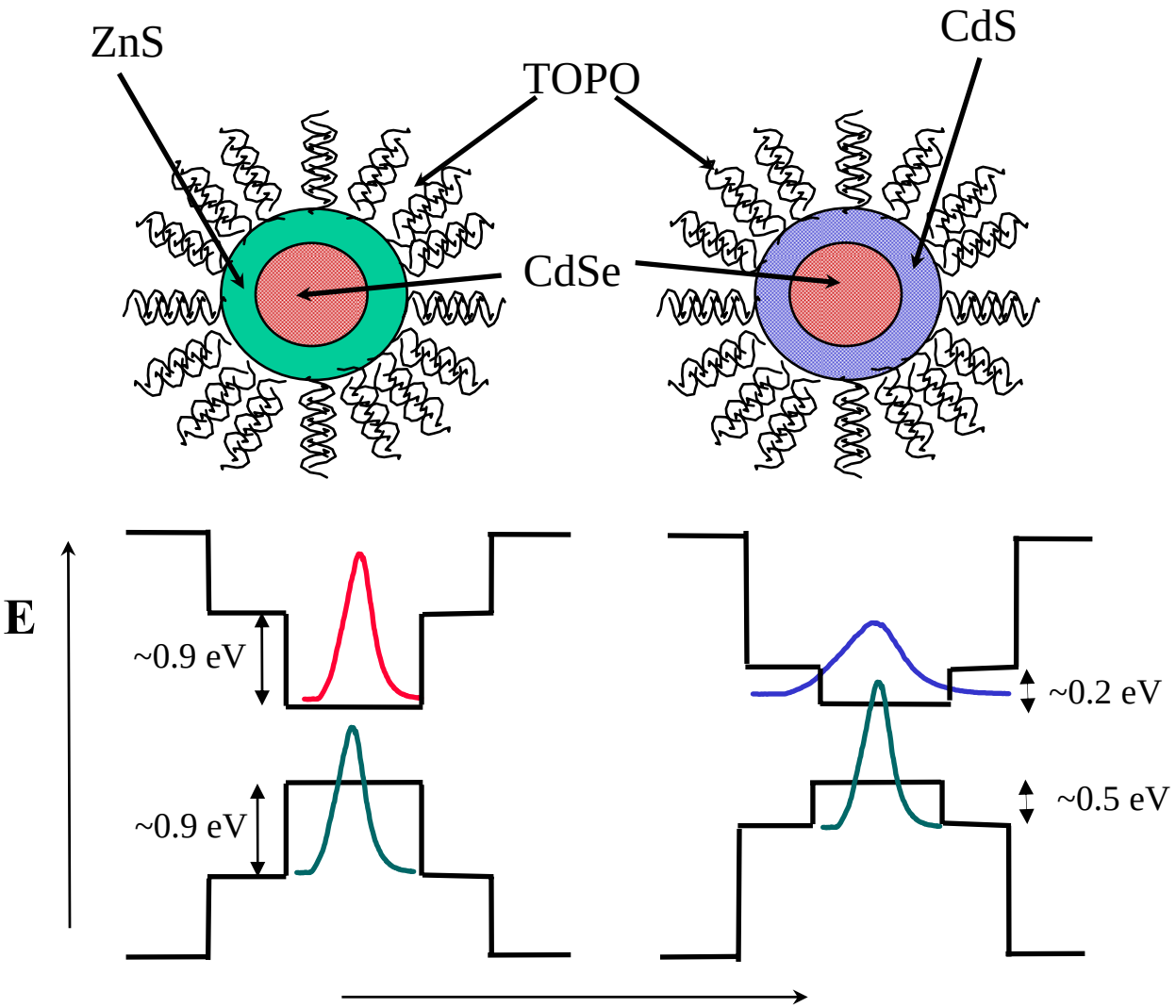

B. O. Dabbousi, *et al.* (1997)

Biological Imaging Applications

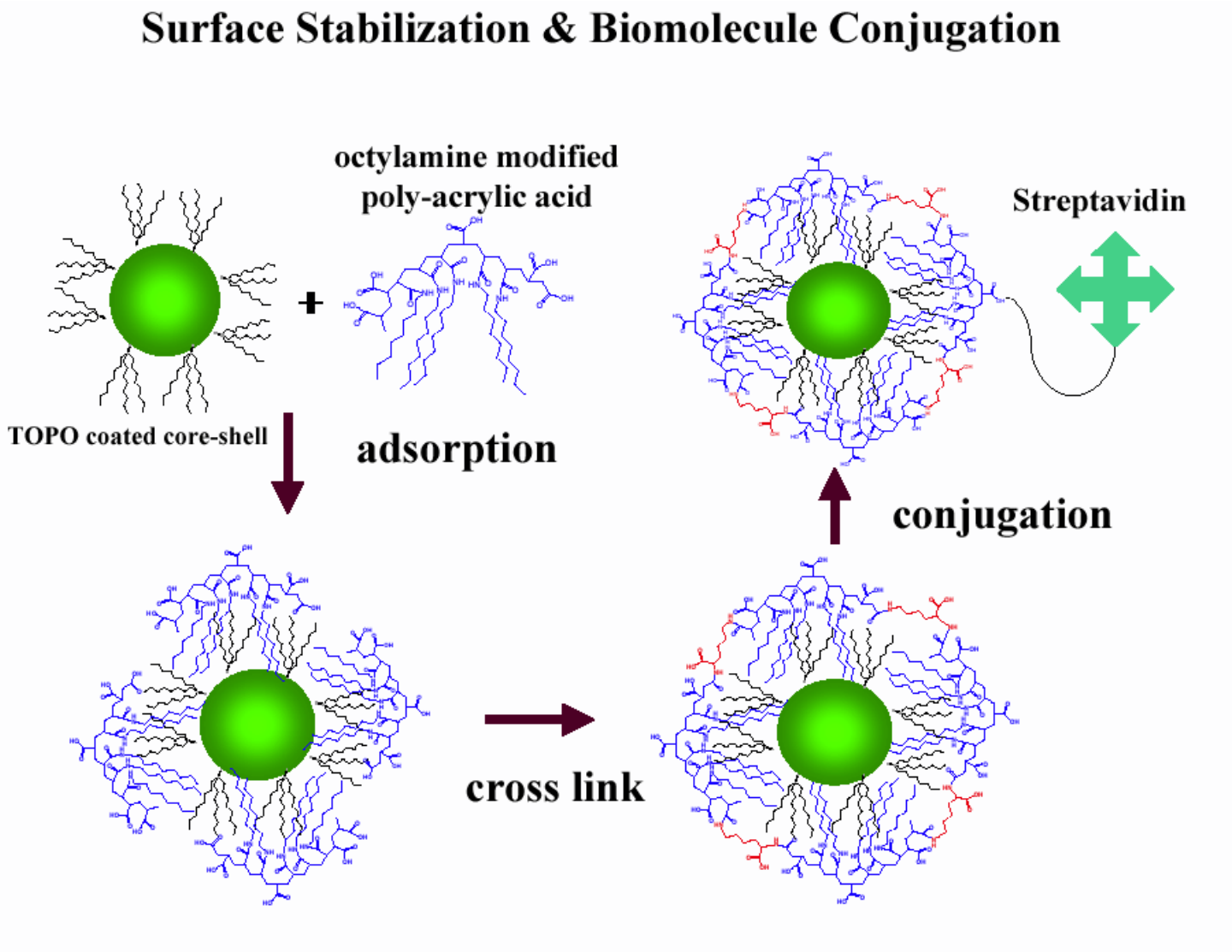

Q Dot Corporation
www.qdots.com

Published in Nature Biotechnology Online

Imaging Mouse Intestine

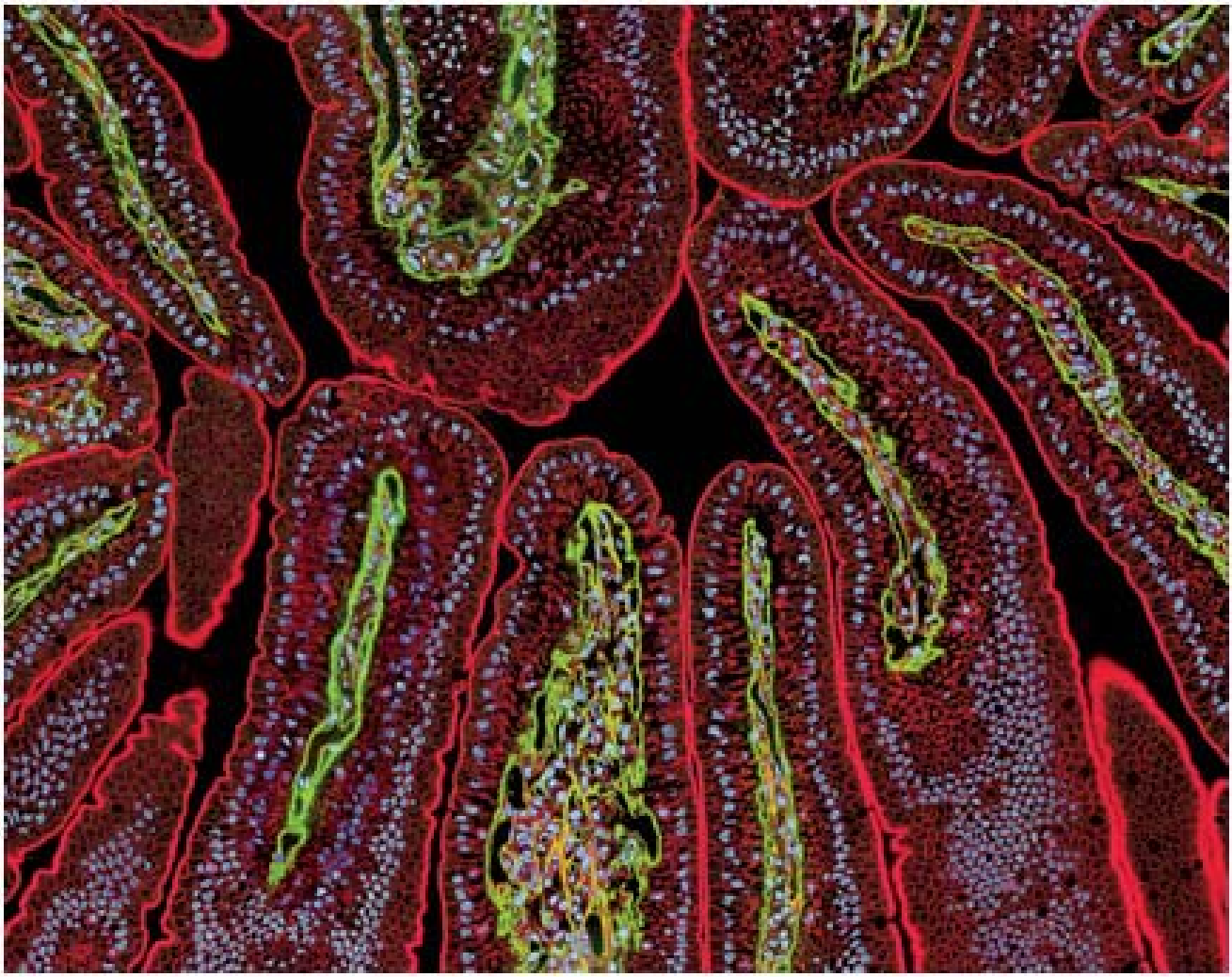

A mouse intestinal section visualized using fluorescent Qdot nanocrystal conjugates. Actin was labeled with a mouse anti-actin monoclonal antibody and visualized using red-fluorescent Qdot 655 goat F(ab')2 anti–mouse IgG (Q11022MP, Q11221MP). Laminin was labeled with a rabbit anti-laminin polyclonal antibody and visualized using green-fluorescent Qdot 525 goat F(ab')2 anti–rabbit IgG (Q11441MP). Nuclei were stained with blue-fluorescent Hoechst 33342 (H1399, H3570, H21492). Image contributed by Thomas Deerinck and Mark Ellisman, The National Center for Microscopy and Imaging Research, San Diego,

Kinetics of Microtubule Motor Steps

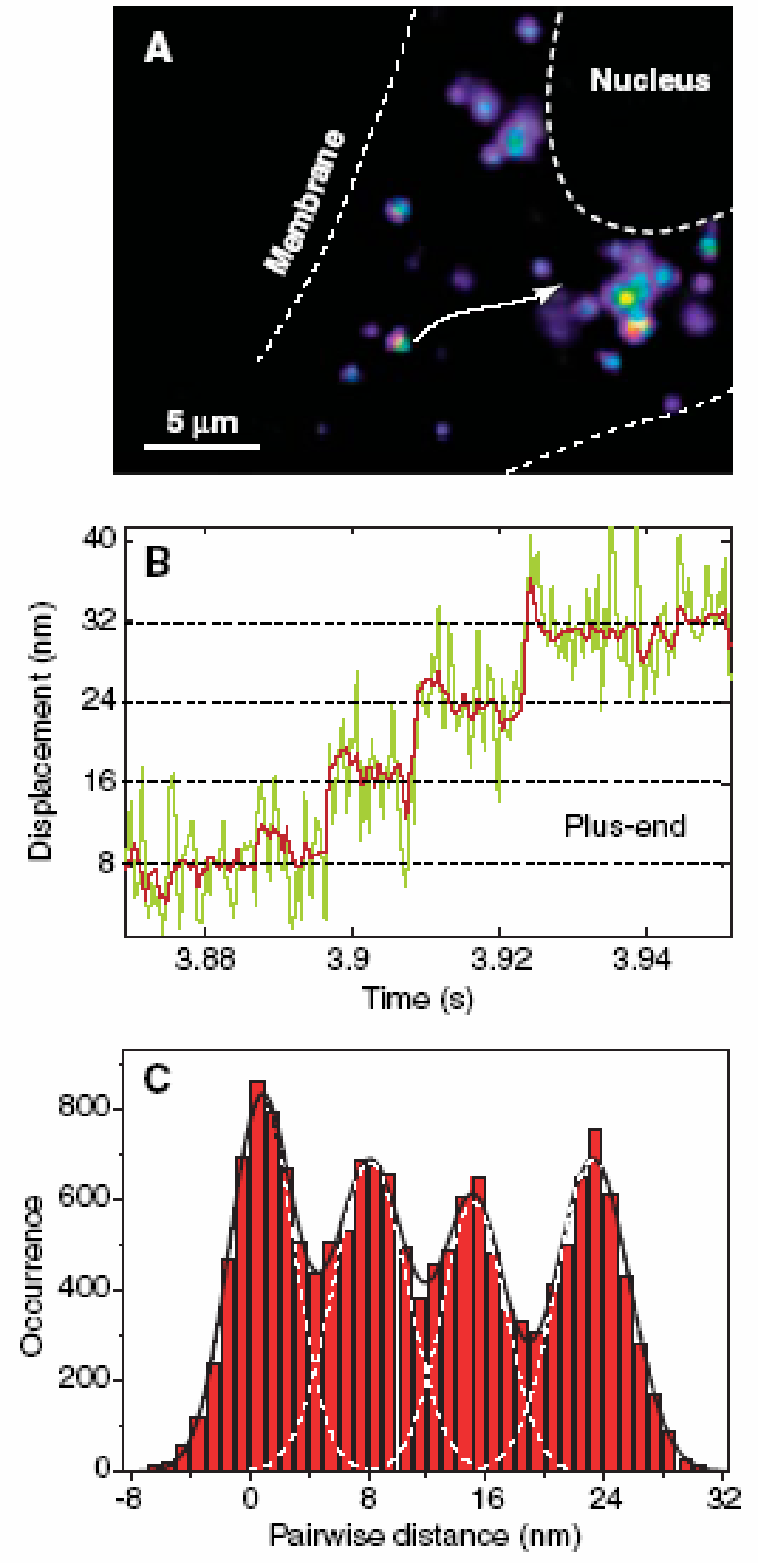

Fig. 2. Observation of individual microtubule motor steps in a live cell with endocytosed quantum dots. (**A**) Live A549 cell with QD-containing endosomes (bright dots), many of which undergo active transport by kinesin (outward movements) or dynein (inward movements, white arrow). (**B**) Displacement trajectory of a outward-going (microtubule plus-end) endosome, exhibiting stepwise movements of the underlying motor (likely kinesin). Green, raw data; red, filtered data. (**C**) Pairwise distance histogram of the filtered displacement trace in (B), with an 8-nm spacing between adjacent peaks.

Sunney Xie etal, Science 312, 228 (2006)

Simple Model for Electronic Structure: Quantum Size Effect

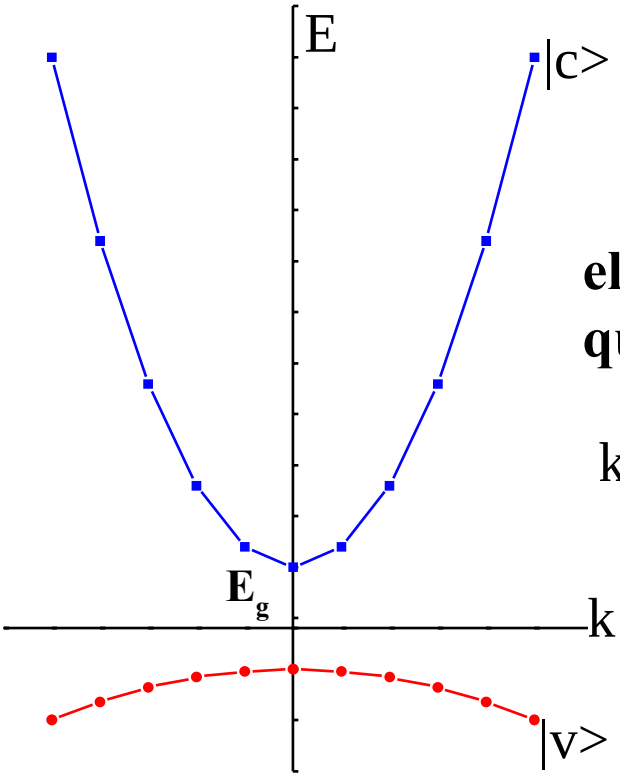

Electron Momentum
$mv=hk=h/\lambda$

electron wavelength λ quantized in particle:

$k \sim n/R$; $n=1,2..$

• Energy of HOMO-LUMO Blue Shifted from bulk band gap

$$E(k) \sim E_g + n^2h^2/(8m_eR^2) + n^2h^2/(8m_hR^2)$$

• Optical Spectra are Discrete and Size Dependent

• Model uses known bulk band structure, and ignores
• bonding reconstruction on surfaces

Quantum Size Effect including Electrostatics

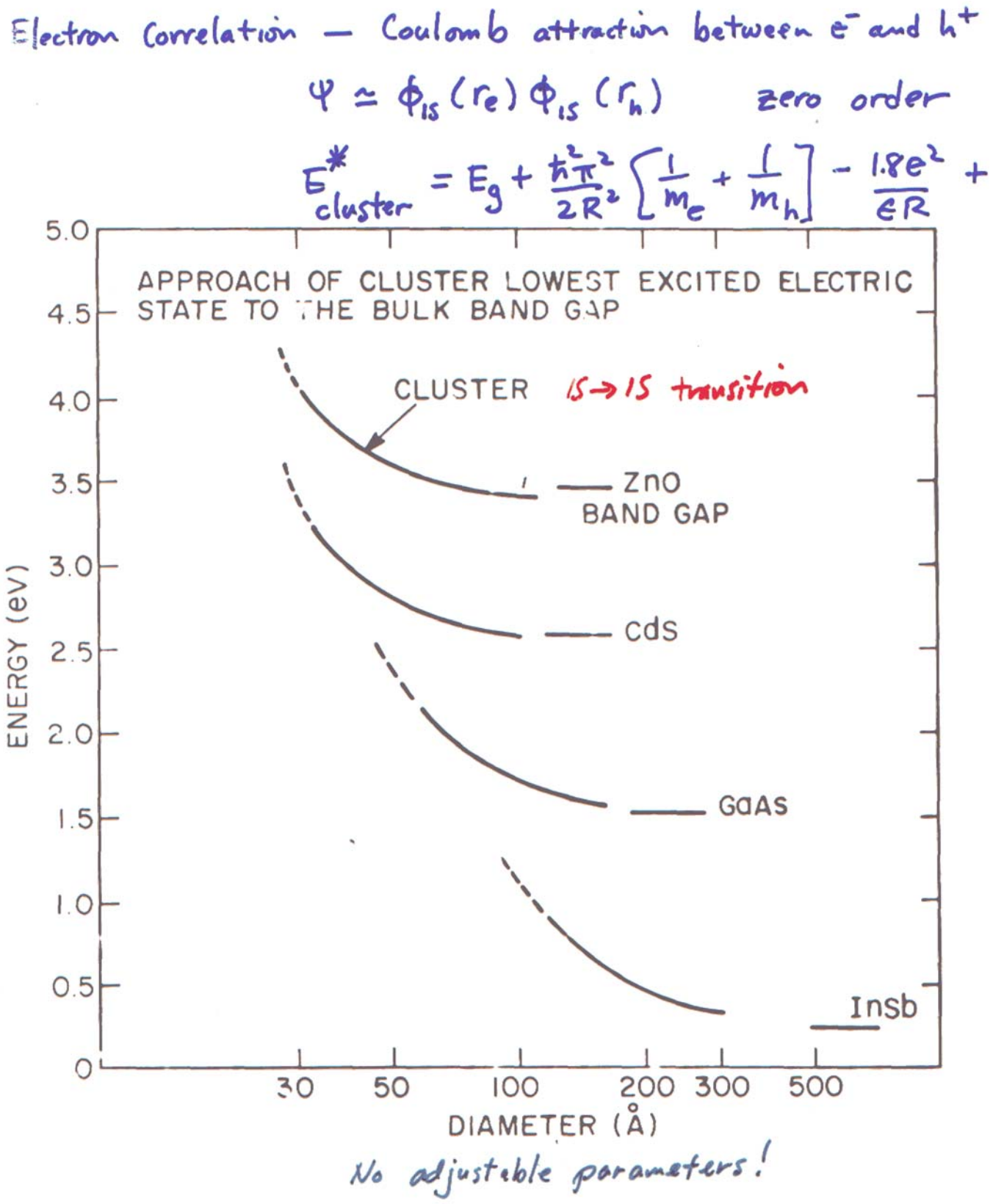

L. Brus, J. Chem. Phys. 79, 5566 (1983); 80, 4403 (1983)

Failure of Quantum Model in Silicon Nanocrystals:

Why does an H passivated 1.3 nm silicon nanocrystal emit in the blue, but an 1.3 nm oxide shell passivated nanocrystal emit in the red?

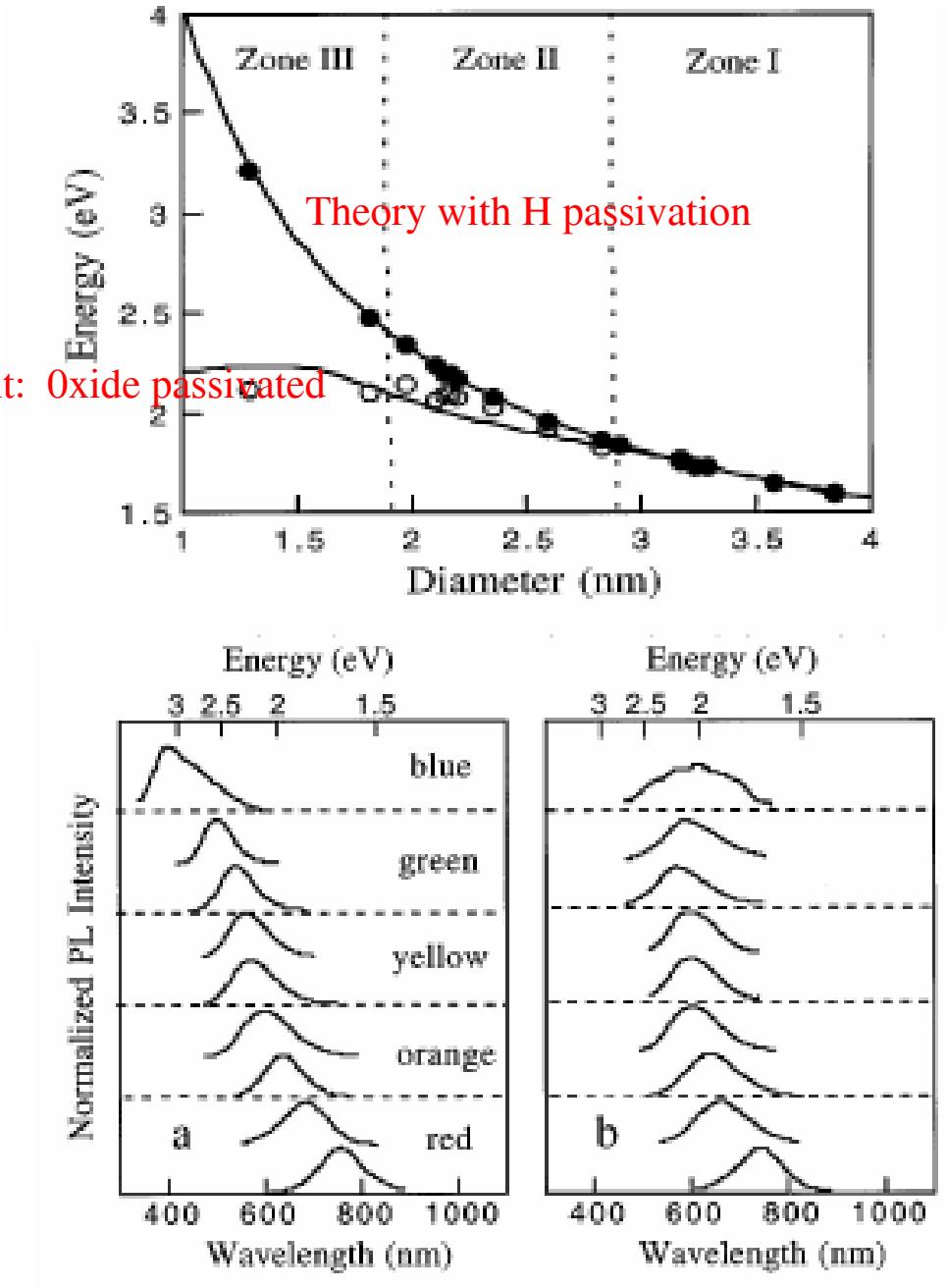

FIG. 1. Room temperature photoluminescence spectra from PSi samples with different porosities kept under Ar atmosphere (a) and after exposure to air (b).

Wolkin etal Phys Rev Lett 82, 197 (1999)

Ab Initio Electronic Structure Calculation

Surface Bonding and Geometrical Optimization
Independent of bulk band structure
Molecular Orbitals extend over entire nanocrystal

Problem: too many atoms

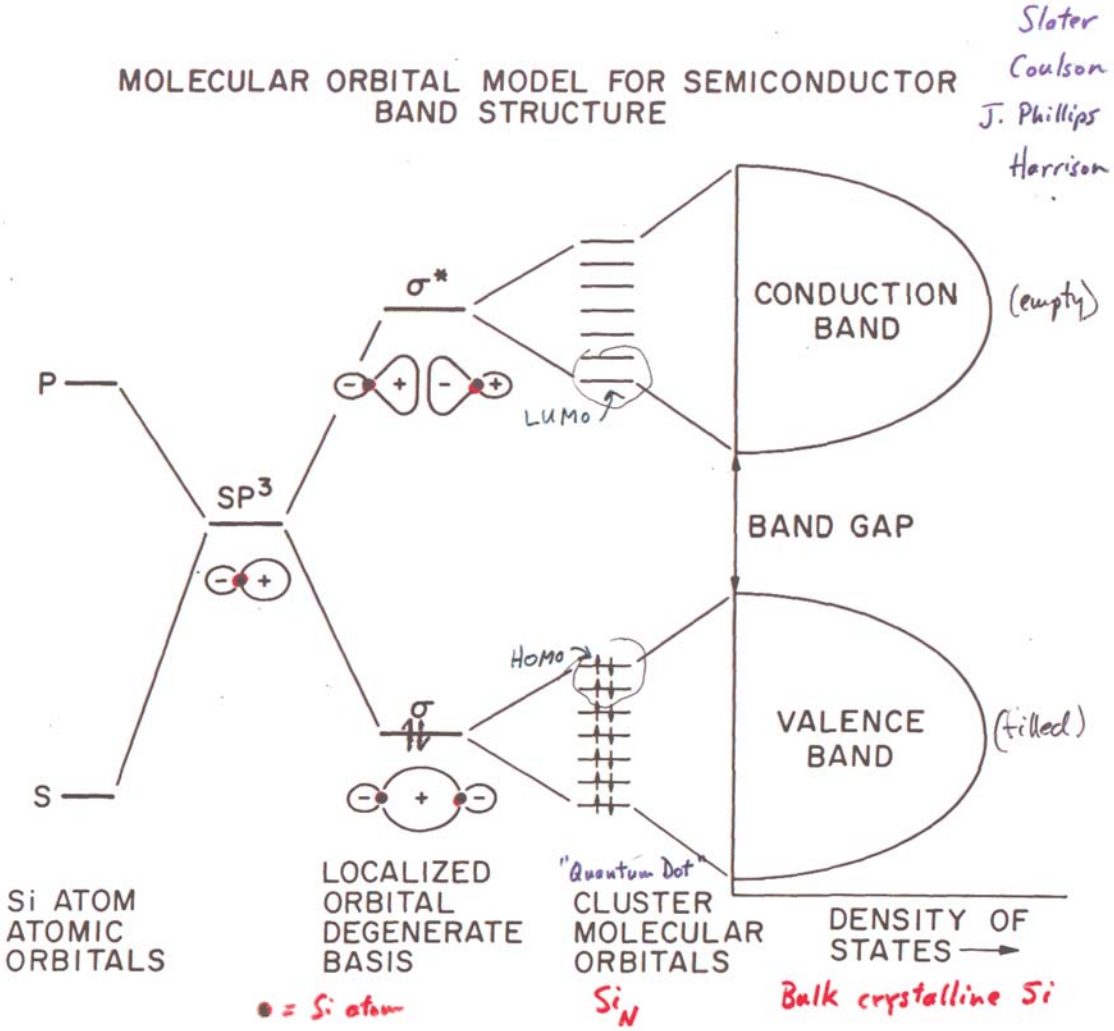

HOMO & LUMO of H-passivated Nanocrystals

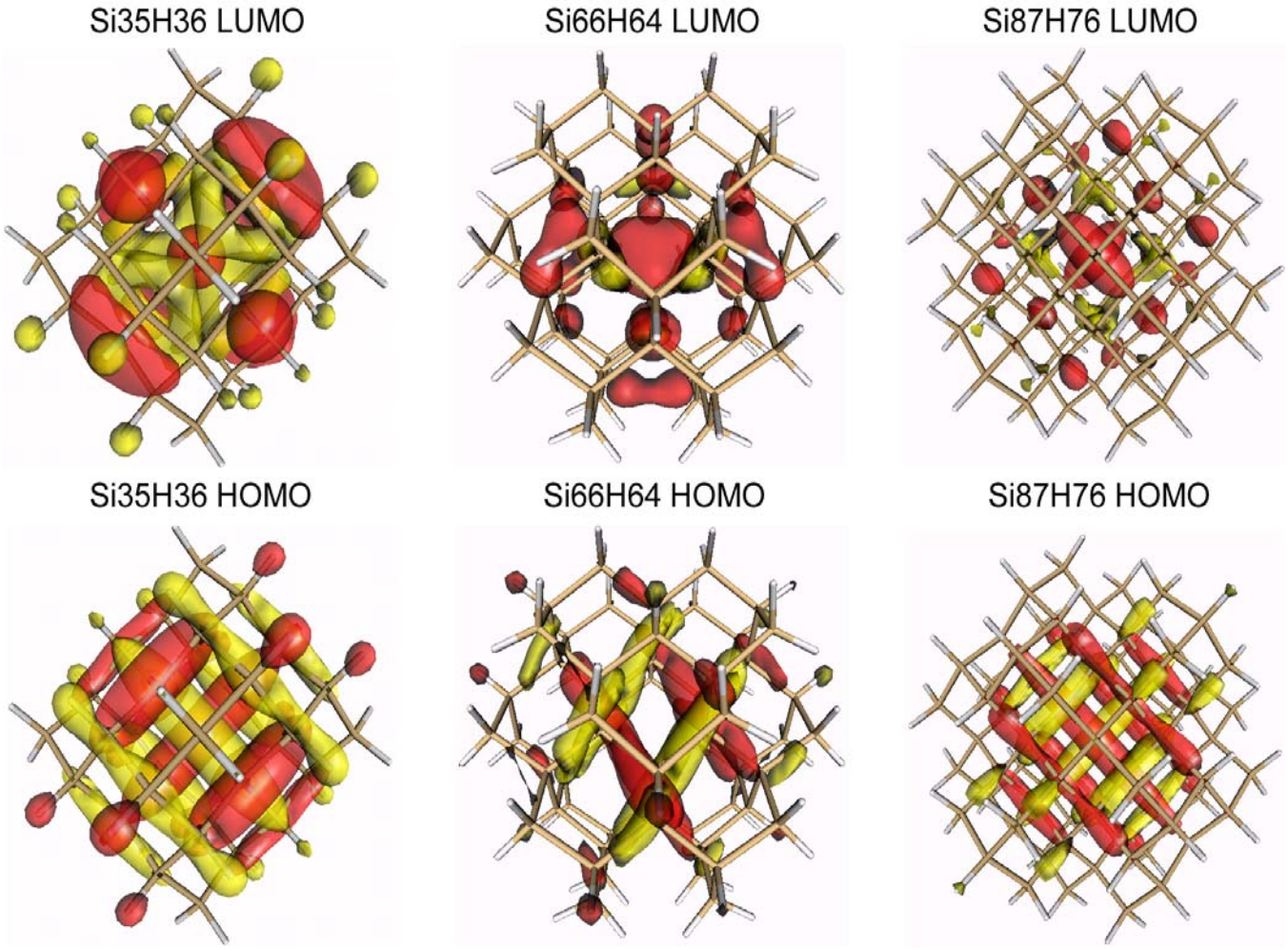

As sizes increases, a 1S orbital with nodes on the surface is formed - expected behavior

Zhou, Friesner, Brus Nanoletters **3**, 163 (2003)
JACS **125**, 15599 (2003)

Molecular Orbitals of Si66 Species

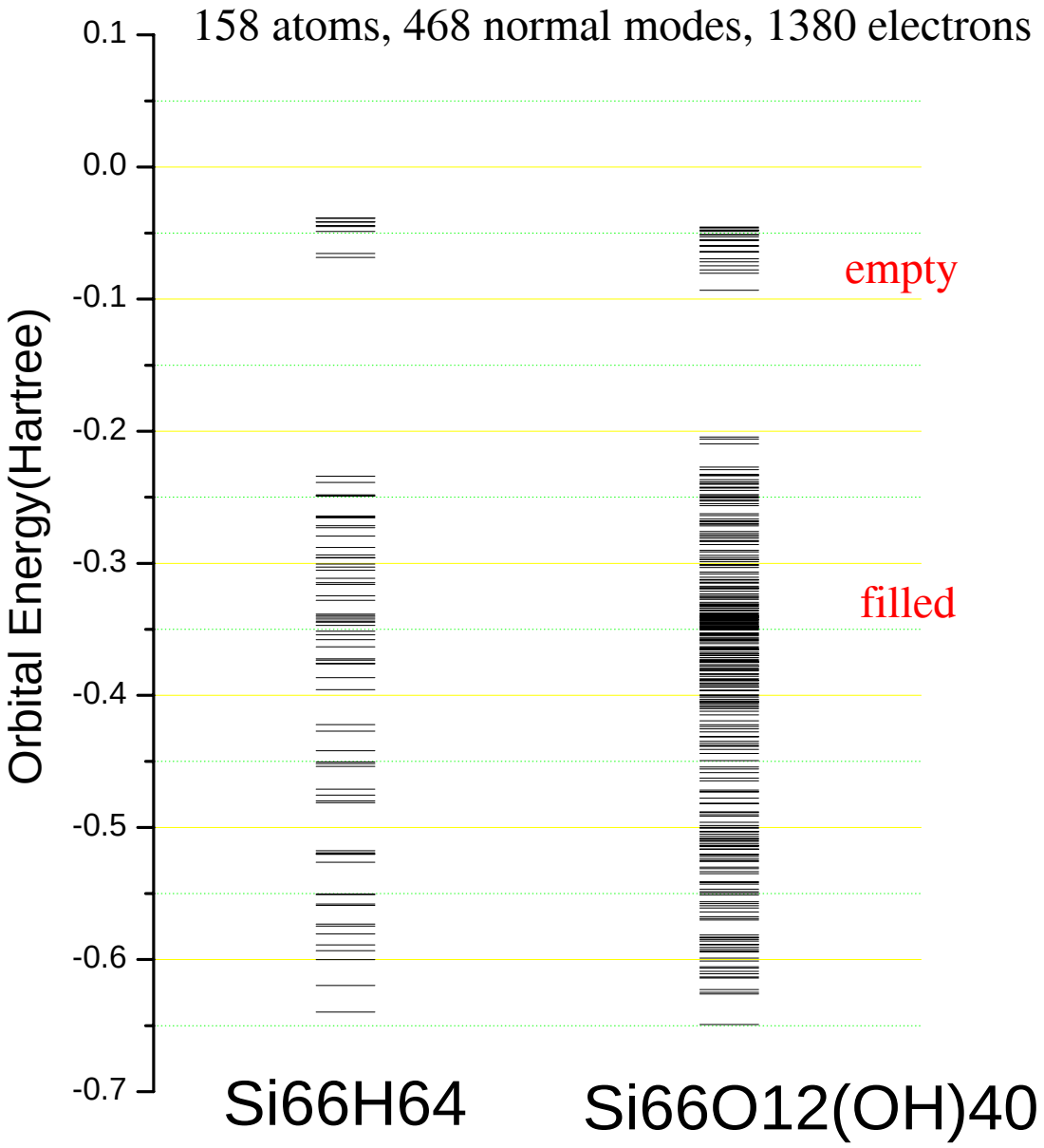

Oxide passivation lowers band gap by 1.5 eV
LUMO moves down
HOMO moves up

Fermi level unchanged; hardness decreases

Si Nanocrystal Band Gap Depends Upon Surface Passivation

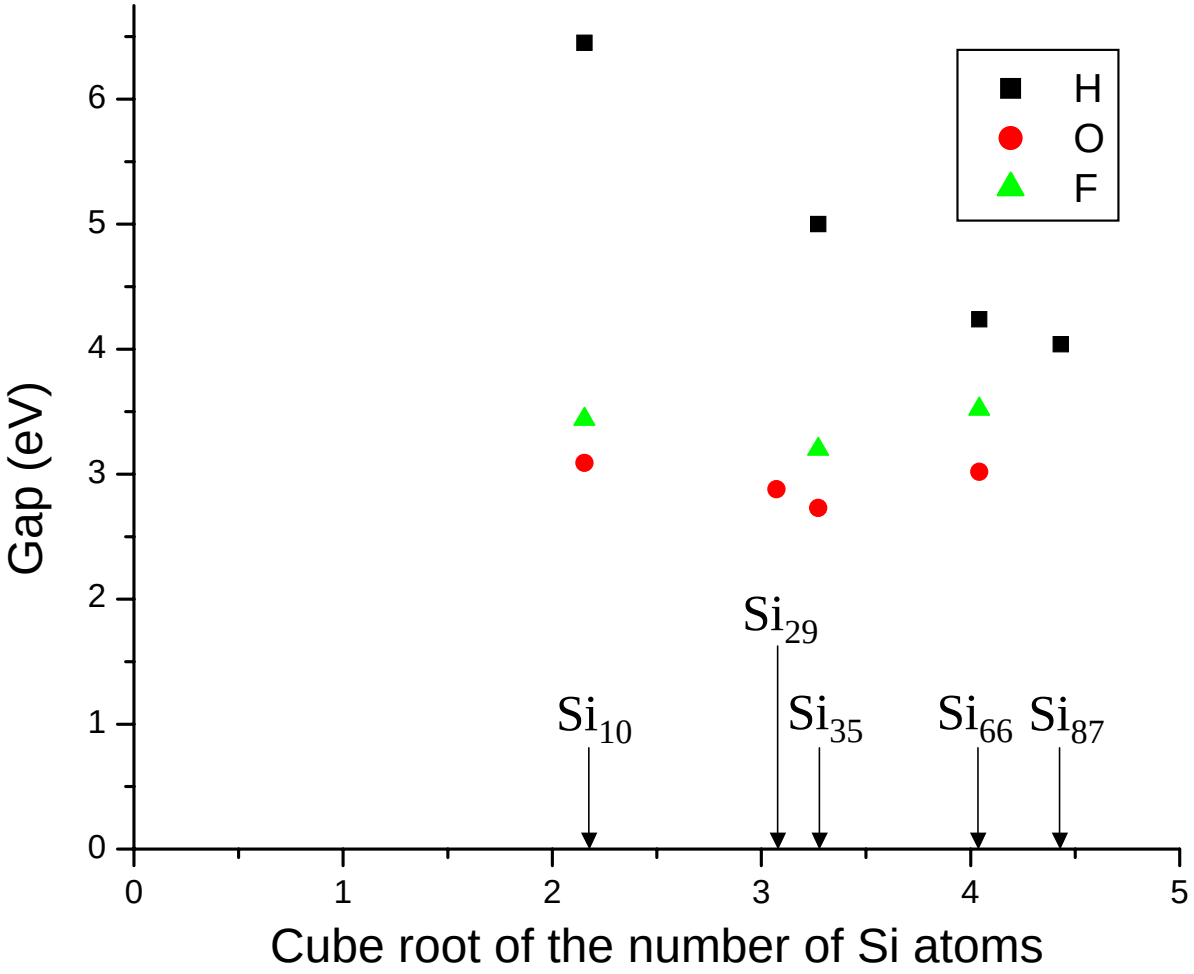

Quantum size effect model works well when electronegativity of capping atom matches that of lattice atom.

CdSe Size Dependent Absorbance

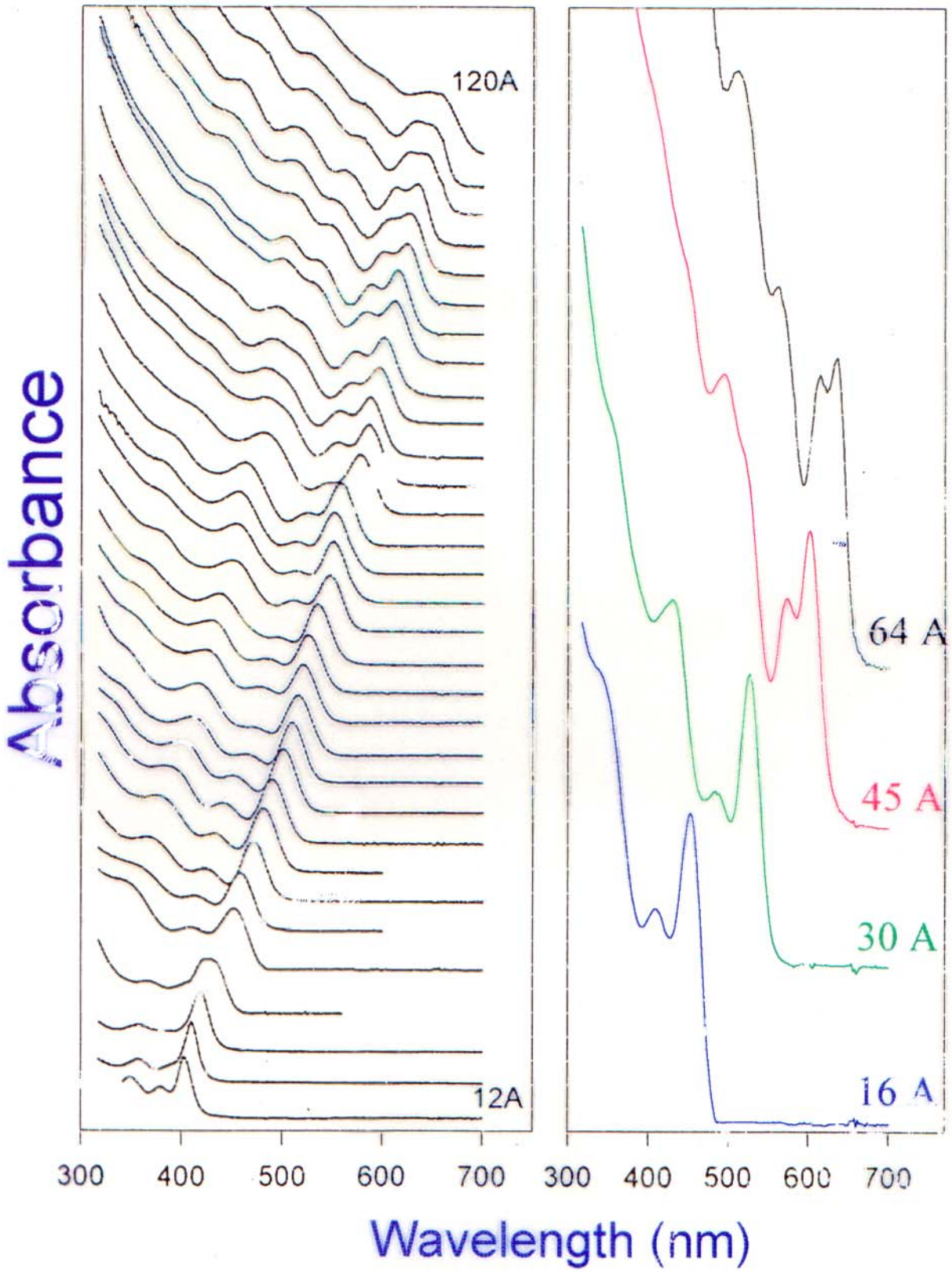

Chris Murray & Moungi Bawendi (MIT)

Bawendi group

How can we observe the band gap luminescence of single nanocrystals?

Nanocrystals have several thousand atoms
Size distribution ca. 5% in diameter
Each nanocrystal is unique
Spectra average over distributions

Experimental Setup: Far-Field Illumination

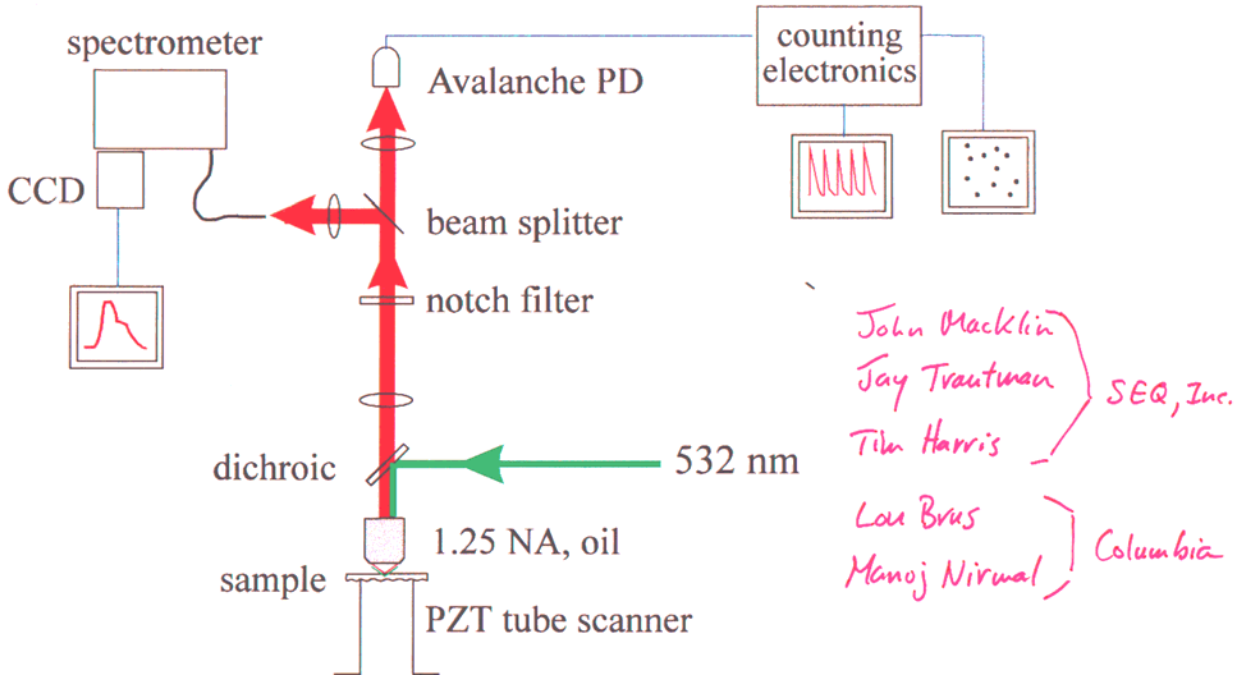

Betzig, Trautman (Bell Labs):
Confocal Scanned Stage Luminescence Spectrometer

Macklin etal, Science 272, 255 (1996)

Random Field of Single Close na ocry ta

cw optical excitation

Raster scan image

field of luminescing nanocrystals

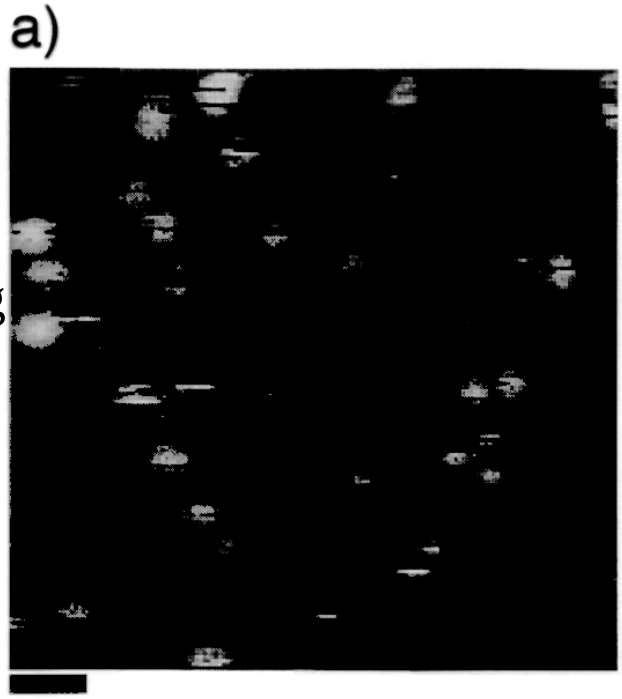

L. in c. ce Ima e

Individual nanocrystals "blink" on and off

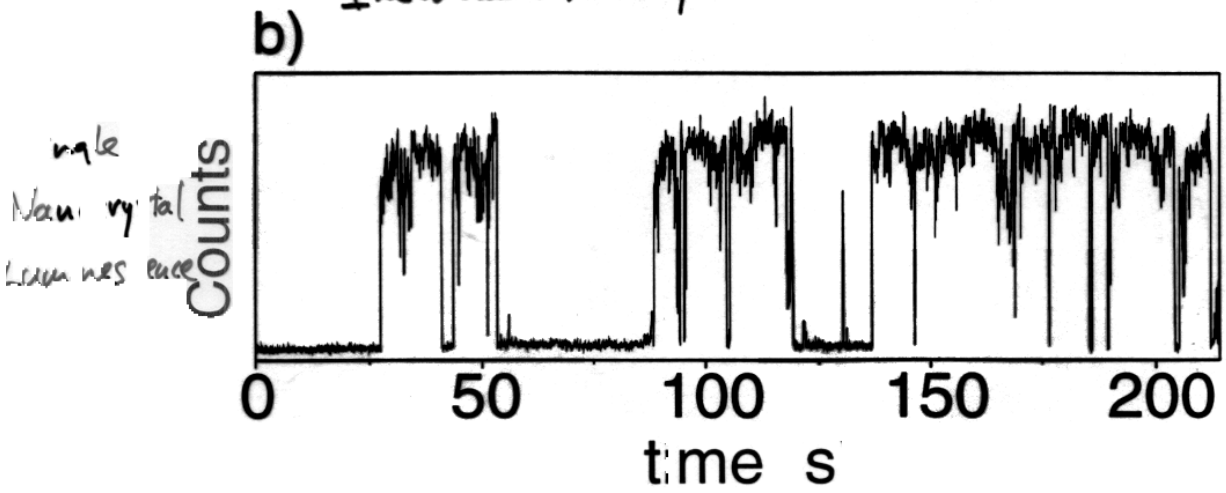

ngle Nan ry tal Lum nes ence

M A rma eta Nat re (a epted for pub catin

Nov 1996 Nat re 383 2(66. ig.

Nirmal etal, Nature 383, 802 (1996)

Schematic Blinking Mechanism: Photoionization and Re-neutralization

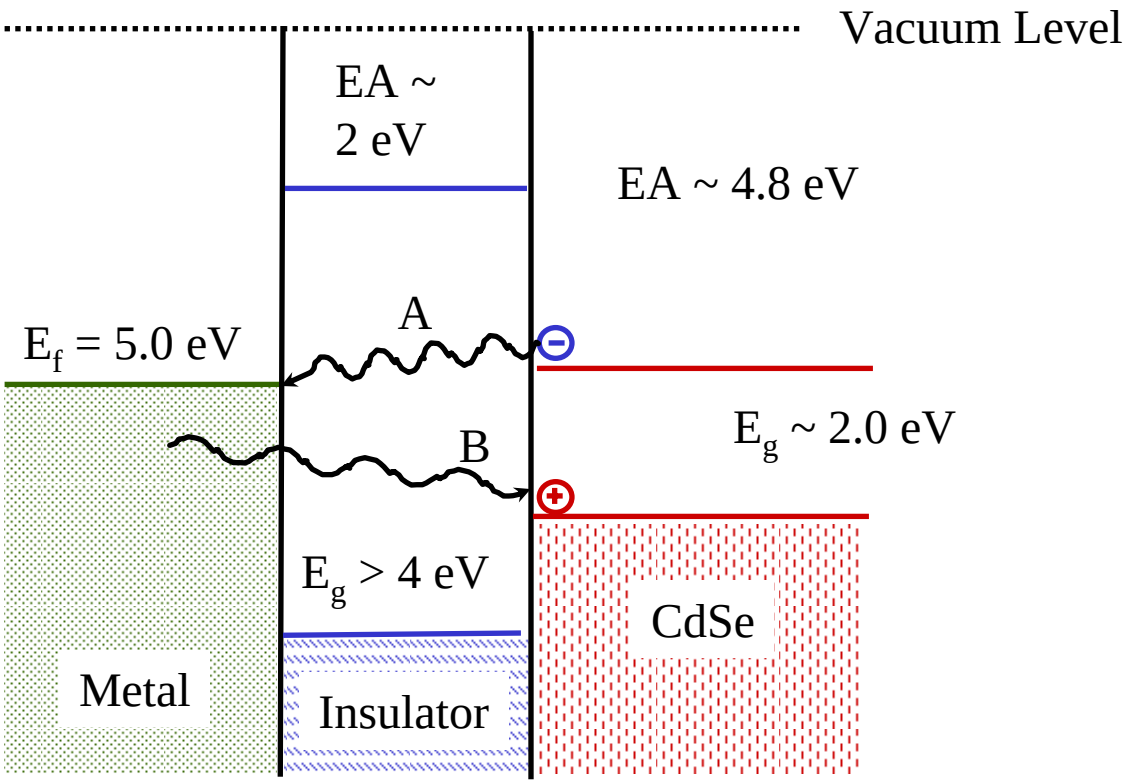

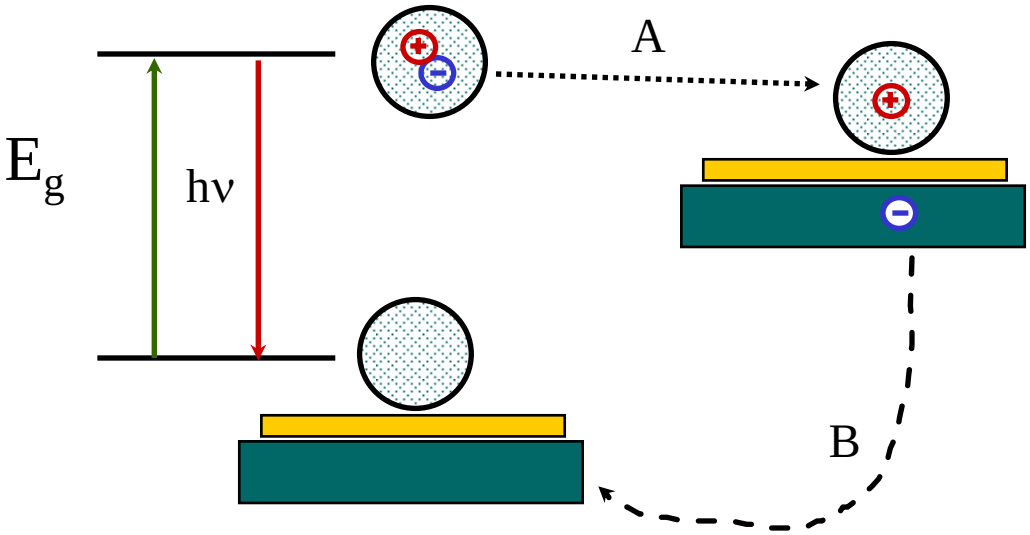

Dark State: Ionized Nanocrystal with hole inside
Bright State: Neutral Nanocrystal

Direct Measurement of Electric Field Due to One Ionized Nanocrystal

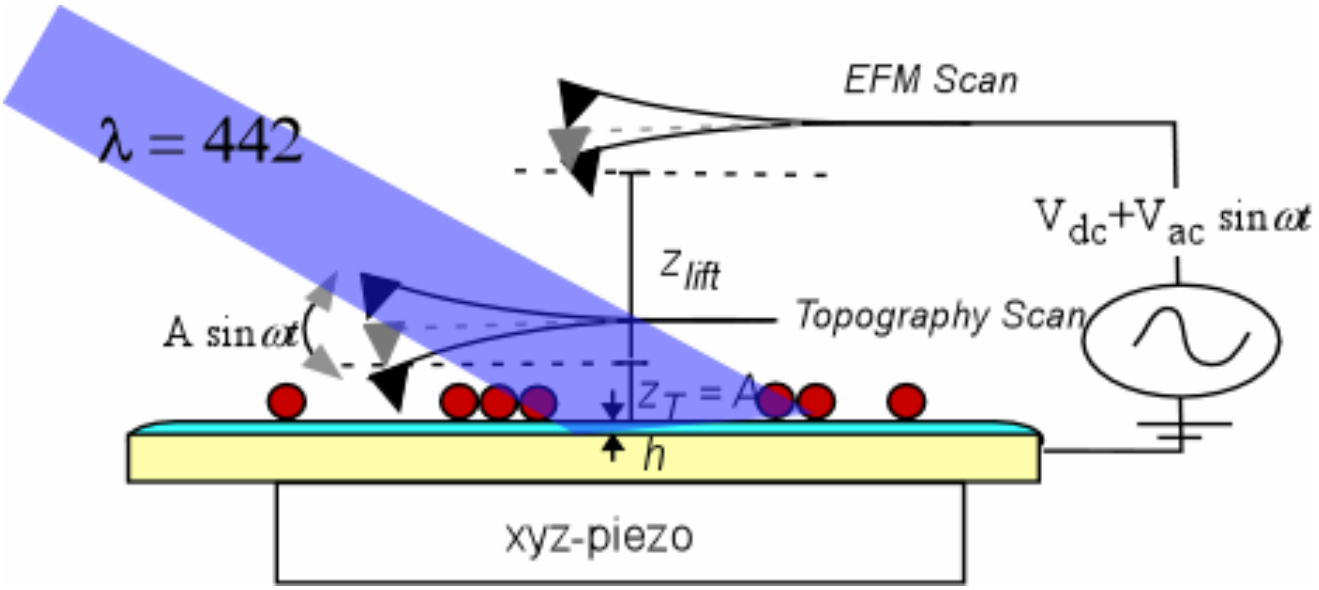

Electric Force Microscopy Invention:

Wickramasinghe IBM

Martin etal, Appl. Phys. Lett. 52, 1103 (1988)E

Can we measure a single charge on a single nanocrystal?

Electric Force Microscopy EFM

Oscillating Capacitor

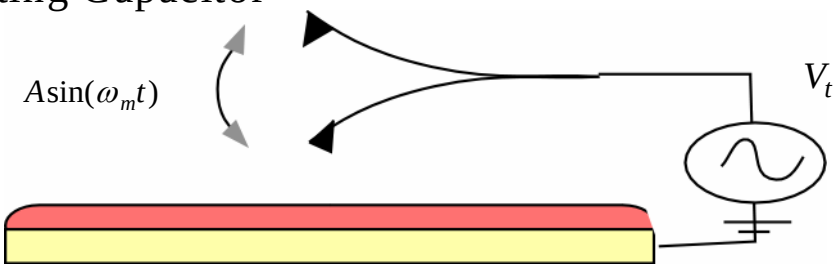

Electrostatic Force $F_{coul} = \frac{Q_1 Q_2}{4\pi\varepsilon z^2}$

Energy Stored in a Capacitor $U = \frac{1}{2}CV^2 = \frac{1}{2}\frac{Q^2}{C}$

Capacitative Force $F = -\frac{dU}{dz} = -\frac{d}{dz}\left(\frac{1}{2}\frac{Q^2}{C}\right) = \frac{1}{2}\frac{Q^2}{C^2}\frac{dC}{dz} = \frac{1}{2}\frac{dC}{dz}V^2$

When a voltage is applied to the tip it feels a sum of electrostatic and capacitative forces. If there are static charges on the surface, image charges are induced in the metal tip.

$$F_e = F_{cap} + F_{coulomb} = \frac{1}{2}\frac{dC}{dz}V^2 + \frac{Q_1 Q_2}{4\pi\varepsilon z^2} \qquad V_{CPD} = (W_{substrate} - W_{tip})/(-e)$$

$$= \frac{1}{2}\frac{dC}{dz}\left((V_{dc} + V_{CPD}) + V_{ac}\sin(\omega t)\right)^2 - \frac{Q_s}{4\pi\varepsilon z}\left(Q_s + CV_{dc} + CV_{ac}\sin(\omega t)\right)$$

$$= \frac{1}{2}\frac{dC}{dz}((V_{dc} + V_{CPD})^2 + \frac{1}{2}V_{ac}^2) - \frac{Q_s}{4\pi\varepsilon z^2}\left(Q_s + C(V_{dc} + V_{CPD})\right)$$

$$+ \underbrace{\left(2(V_{dc} + V_{CPD})\frac{dC}{dz} - \frac{Q_s C}{4\pi\varepsilon z^2}\right)V_{ac}\sin(\omega t)}_{F(\omega)} + \underbrace{\frac{1}{4}\frac{dC}{dz}V_{ac}^2}_{F(2\omega)}\cos(2\omega t)$$

CdSe/ZnS Charge Blinking on Graphite

Krauss etal J. Phys. Chem. 2001, B105, 1725

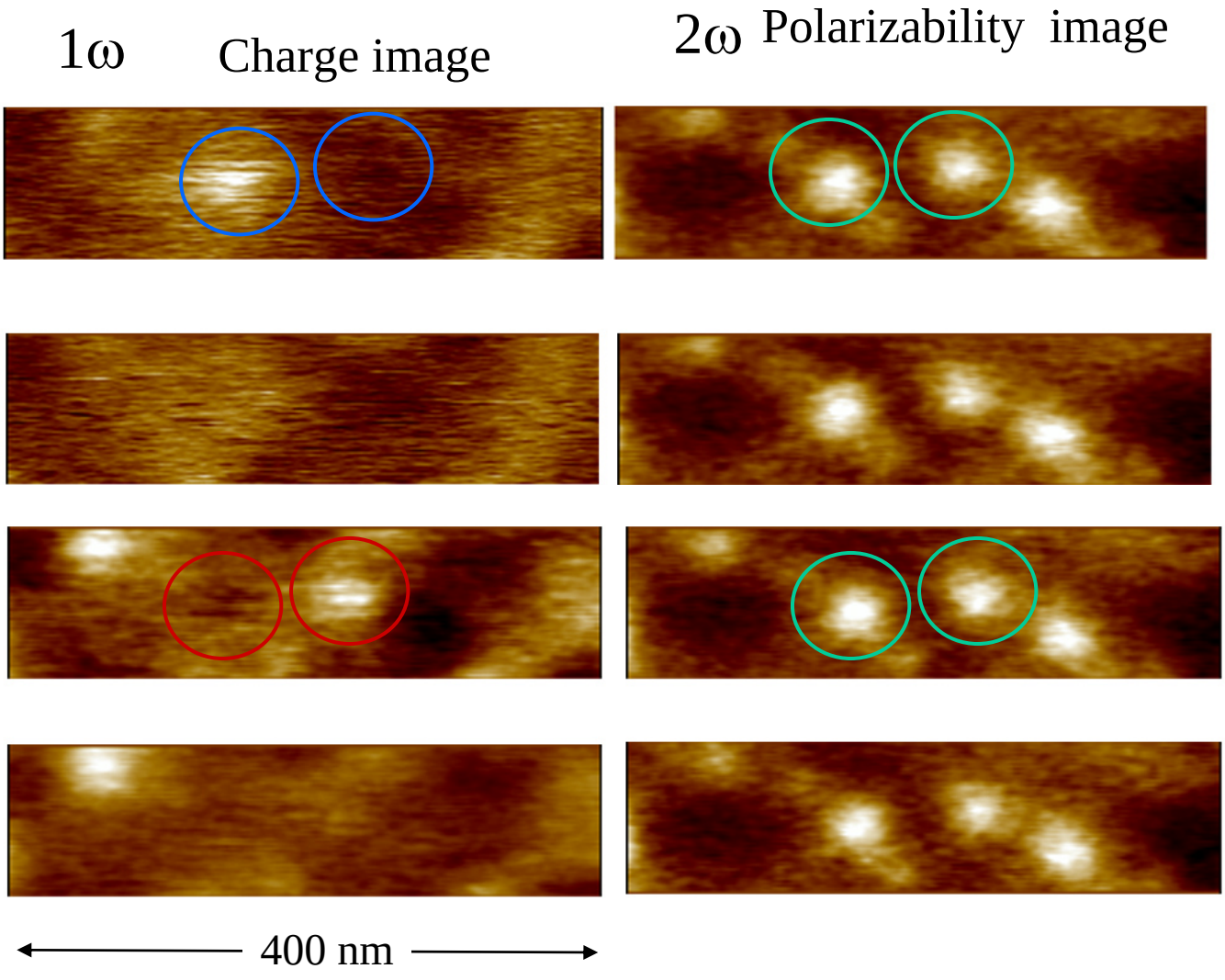

• Illuminated with 20 W/cm^2 at 442 nm

•Direct observation of Charge Blinking provides evidence for photoionization mechanism of Luminescence Blinking

Physical Size Regimes for Semiconductor Nanocrystals

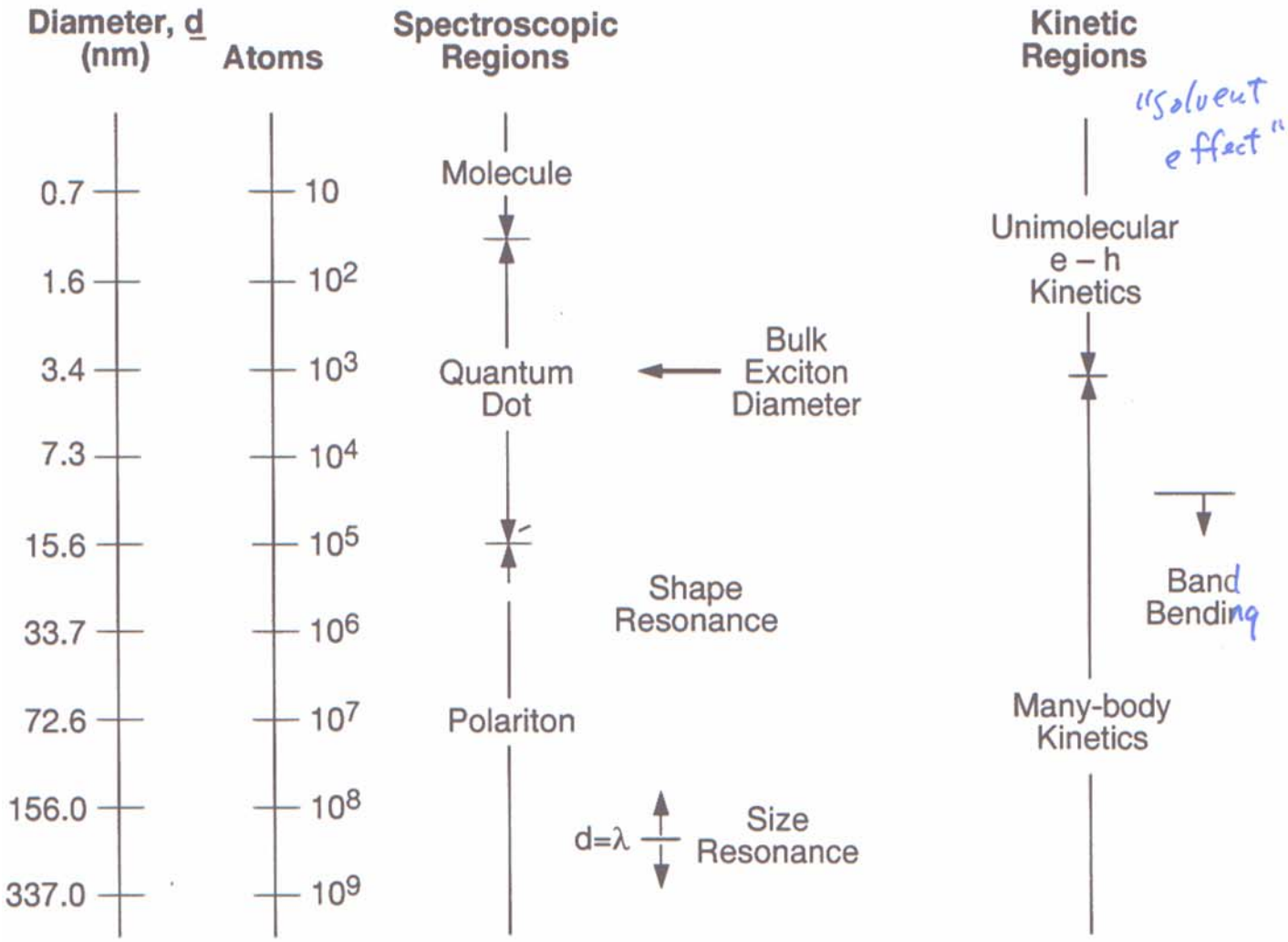

Evolution from molecules to solid state as size increases

MH4M20543.4